

Decay $B \rightarrow K^*(\rightarrow K\pi)\ell^+\ell^-$ in covariant quark model

S. Dubnička,¹ A.Z. Dubničková,² N. Habył,^{3,*}

M.A. Ivanov,^{4,†} A. Liptaj,^{1,‡} and G.S. Nurbakova^{3,§}

¹*Institute of Physics, Slovak Academy of Sciences, Bratislava, Slovakia*

²*Comenius University, Bratislava, Slovakia*

³*Al-Farabi Kazakh National University, Almaty, Kazakhstan*

⁴*Joint Institute for Nuclear Research, Dubna, Russia*

Abstract

Our article is devoted to the study of the rare $B \rightarrow K^*\ell^+\ell^-$ decay where $\ell = e, \mu, \tau$. We compute the relevant form factors in the framework of the covariant quark model with infrared confinement in the full kinematical momentum transfer region. The calculated form factors are used to evaluate branching fractions and polarization observables in the cascade decay $B \rightarrow K^*(\rightarrow K\pi)\ell^+\ell^-$. We compare the obtained results with available experimental data and the results from other theoretical approaches.

PACS numbers:

Keywords: relativistic quark model, confinement, B-meson, decay widths, polarization observables

*Electronic address: nuigui@mail.ru

†Electronic address: ivanovm@theor.jinr.ru

‡Electronic address: andrej.liptaj@gmail.com

§Electronic address: guliya.nurbakova@mail.ru

I. INTRODUCTION

The rare flavour changing neutral current (FCNC) decays are forbidden in the Standard Model (SM) at the tree level. They proceed only via loops in the perturbation theory. For this reason, these decays are sensitive to possible effects of new physics beyond the SM. New heavy particles can contribute to the branching fractions and the angular decay distributions.

It is generally believed that the decay mode $B \rightarrow K^*(\rightarrow K\pi)\mu^+\mu^-$ is one of the best modes to search for new physics beyond the SM. The angular distribution makes possible an independent measurement of several observables as a function of the dilepton invariant mass. A large number of observables obtained in this manner allows for unique tests of the SM contributions (see the recent experimental review [1]). A deviation of 3.3σ is seen in e.g. $R(D^*) \equiv \mathcal{B}(B^- \rightarrow D^*\tau^-\bar{\nu}_\tau)/\mathcal{B}(B^- \rightarrow D^*\ell^-\bar{\nu}_\ell)$ with $R(D^*)|_{\text{expt}} = 0.321 \pm 0.021$ [2] and $R(D^*)|_{\text{SM}} = 0.252 \pm 0.003$ [3–6]. An analogous result questioning the lepton flavour universality exists also for $B \rightarrow K$ decays by Belle [7].

The results of a measurement of form-factor independent angular observables in the decay $B^0 \rightarrow K^{*0}(892)\mu^+\mu^-$ were presented in [8]. The analysis is based on a data sample corresponding to an integrated luminosity of 1.0 fb^{-1} , collected by the LHCb experiment in $p\bar{p}$ collisions at a center-of-mass energy of 7 TeV. Four observables are measured in six bins of the dimuon invariant mass squared, q^2 , in the range $0.1 < q^2 < 19.0 \text{ GeV}^2$. Agreement with the SM predictions is found for 23 of the 24 measurements. A local discrepancy, corresponding to 3.7 standard deviations, is observed in one q^2 bin for one of the observables.

The measurements were followed by a large number of publications, with many different scenarios analyzed [9]–[46]. Several authors discuss an appropriate choice of observables with small model dependence, which would discriminate between SM and new physics. Other authors use various assumptions or models to evaluate form factors or study Wilson coefficients (and related operators) in order to make theoretical predictions and, possibly, argue whether the observed deviations do or do not favor a beyond SM explanation.

Our article is devoted to the study of the $B \rightarrow K^*\ell^+\ell^-$ decay, first, to evaluate the relevant form factors in the framework of the covariant quark model with infrared confinement, and, second, to demonstrate the equivalence of our helicity-based approach with approaches of other authors for what concerns the model independent four-fold angular decay distribution

and related results. Form factors are then exploited for evaluation of physical observables. The first paper in this direction has been published in 2002, Ref. [49]. It was one of the first paper where the full four-fold angular decay distribution has been derived for this process in terms of helicity amplitudes including lepton mass effects. However, our model in that time was suffering from lack the of confinement that restricted the range of applications to the hadrons (mesons and baryons) which satisfy the so-called "threshold inequality": the hadron mass should be smaller then the total mass of its constituents, i.e. the sum of the constituent quark masses. In this vein, our model was successfully developed for the study of light hadrons (e.g., pion, kaon, baryon octet, Δ -resonance), heavy-light hadrons (e.g., D , D_s , B and B_s -mesons, Λ_Q , Σ_Q , Ξ_Q and Ω_Q -baryons) and double heavy hadrons (e.g, J/Ψ , Υ and B_c -mesons, Ξ_{QQ} and Ω_{QQ} baryons). To extend our approach to other hadrons we had to introduce extra model parameters or do some approximations, like, e.g., to introduce a cutoff parameter for external hadron momenta to guarantee the fulfilment of the above mentioned "threshold inequality". Therefore, at that stage we were unable to apply our approach to the study of rare decays involving K^* mesons. The numerical results for the physical observables were presented in [49] only for decays $B \rightarrow K\ell^+\ell^-$, $B_c \rightarrow D\ell^+\ell^-$ and $B_c \rightarrow D^*(\rightarrow D\pi)\ell^+\ell^-$.

Our relativistic constituent quark model has been refined in 2009, see Ref. [50], where the confinement of quarks was implemented. It was done, first, by introducing the scale integration in the space of α -parameters, and, second, by cutting this scale integration on the upper limit which corresponds to an infrared cutoff. In this manner one removes all possible thresholds present in the initial quark diagram. The cutoff parameter is taken to be the same for all physical processes. Other model parameters were adjusted by fitting the calculated quantities of the basic physical processes to available experimental data. As an application, the electromagnetic form factors of the pion and the transition form factors of the omega and eta Dalitz decays have been calculated.

New values for the parameters of the covariant constituent quark model with built-in infrared confinement have been determined in [51] by a fit to the leptonic decay constants and a number of electromagnetic decays. Then the form factors of the $B(B_s) \rightarrow P(V)$ transitions were evaluated in the full kinematical region of momentum transfer squared in a parameter free way.

The model was than applied to a wide range of nonleptonic and semileptonic meson de-

cays, e.g. [52, 53] and it was extended also to the baryon sector [54–58]. Different observables related to (nucleons and) heavy Λ baryons were calculated in [54–56, 58]. Furthermore, the consequences of treating the $X(3872)$ meson as a tetraquark bound state were explored in Refs. [59, 60]. Some of the above research was collected in the review [61].

Our paper is organized as follows. In Sec. II we review salient features of the covariant quark model. In Sec. III we present the calculated form factors in the full kinematical momentum transfer region. In Sec. IV we discuss the effective Hamiltonian, matrix elements, invariant and helicity form factors. Sec. V is devoted to the four-fold angular decay distribution in the cascade decay $B \rightarrow K^*(\rightarrow K\pi)\bar{\ell}\ell$ and, in particular, to the relation of our helicity formalism with an approach based on the transversality amplitudes which is widely used by both experimentalists and theorists. In Sec. VI we present our numerical results on the branching fractions, forward-backward asymmetry, longitudinal polarization and a set of the so-called “clean” observables P_i which depend on the hadron uncertainties (form factors) in a minimal way. Finally, in Sec. VII we summarize our results.

II. THEORETICAL FRAMEWORK

The covariant confined quark model developed in [49, 50, 62, 63] has been applied to a large number of elementary particle processes. This model can be viewed as an effective quantum field approach to hadronic interactions based on an interaction Lagrangian of hadrons interacting with their constituent quarks. The coupling strength is determined by the compositeness condition $Z_H = 0$ where Z_H is the wave function renormalization constant of the hadron. The hadron field renormalization constant Z_H characterizes the overlap between the bare hadron field and the bound state formed from the constituents. Once this constant is set to zero, the dynamics of hadron interactions is fully described by constituent quarks in quark loop diagrams with local constituent quark propagators. Matrix elements are generated by a set of quark loop diagrams according to the $1/N_c$ expansion. The ultraviolet divergences of the quark loops are regularized by including vertex functions for the hadron-quark vertices which, in addition, describe finite size effects due to the non-pointlike structure of hadrons. Quark confinement was implemented into the model [50] by introducing an infrared cutoff on the upper limit of the scale integration to avoid the appearance of singularities in any matrix element. The infrared cutoff parameter λ is taken

to have a common value for all processes. The covariant confined quark model contains only a few model parameters: the light and heavy constituent quark masses, the size parameters that describe the size of the distribution of the constituent quarks inside the hadron and the infrared cutoff parameter λ . They are determined by a fit to available experimental data.

A. Effective Lagrangian

The coupling of a meson $M(q_1\bar{q}_2)$ to its constituent quarks q_1 and \bar{q}_2 is described by the Lagrangian

$$\mathcal{L}_{\text{int}}(x) = g_M M(x) \int dx_1 \int dx_2 F_M(x, x_1, x_2) \bar{q}_2(x_2) \Gamma_M q_1(x_1) + \text{h.c.} \quad (1)$$

Here, Γ_M is a Dirac matrix which projects onto the spin quantum number of the meson field $M(x)$. The function F_M is related to the scalar part of the Bethe-Salpeter amplitude and characterizes the finite size of the meson. To satisfy translational invariance the function F_H has to fulfill the identity $F_M(x+a, x_1+a, x_2+a) = F_M(x, x_1, x_2)$ for any four-vector a . In the following we use a specific form for the scalar vertex function

$$F_M(x, x_1, x_2) = \delta(x - w_1 x_1 - w_2 x_2) \Phi_M((x_1 - x_2)^2), \quad (2)$$

where Φ_M is the correlation function of the two constituent quarks with masses m_{q_1} , m_{q_2} and the mass ratios $w_i = m_{q_i}/(m_{q_1} + m_{q_2})$.

We choose a simple Gaussian form of the vertex function $\bar{\Phi}_M(-k^2)$. The minus sign in the argument of this function is chosen to emphasize that we are working in the Minkowski space. One has

$$\bar{\Phi}_M(-k^2) = \exp(k^2/\Lambda_M^2), \quad (3)$$

where the parameter Λ_M characterizes the size of the meson. Since k^2 turns into $-k_E^2$ in the Euclidean space, the form (3) has the appropriate fall-off behavior in the Euclidean region. We emphasize that any choice for Φ_M is appropriate as long as it falls off sufficiently fast in the ultraviolet region of the Euclidean space to render the corresponding Feynman diagrams ultraviolet finite. We choose a Gaussian form for Φ_M for calculational convenience.

B. Compositeness condition

The coupling constant g_M in Eq. (1) is determined by the so-called *compositeness condition* suggested by Weinberg [64] and Salam [65] (for a review, see Ref. [66]) and extensively used in our studies (for details, see Ref. [63]). The compositeness condition requires that the renormalization constant Z_M of the elementary meson field $M(x)$ is set to zero, i.e.,

$$Z_M = 1 - \frac{3g_M^2}{4\pi^2} \bar{\Pi}'_M(m_M^2) = 0, \quad (4)$$

where $\bar{\Pi}'_H$ is the derivative of the meson mass operator. To clarify the physical meaning of the compositeness condition in Eq. (4), we first want to remind the reader that the renormalization constant $Z_M^{1/2}$ can be also interpreted as the matrix element between the physical and the corresponding bare state. The condition $Z_M = 0$ implies that the physical state does not contain the bare state and is appropriately described as a bound state. The interaction Lagrangian of Eq. (1) and the corresponding free parts of the Lagrangian describe both the constituents (quarks) and the physical particles (hadrons) which are viewed as the bound states of the quarks. As a result of the interaction, the physical particle is dressed, i.e. its mass and wave function have to be renormalized. The condition $Z_M = 0$ also effectively excludes the constituent degrees of freedom from the space of physical states. It thereby guarantees that there is no double counting for the physical observable under consideration. The constituents exist only in virtual states. One of the corollaries of the compositeness condition is the absence of a direct interaction of the dressed charged particle with the electromagnetic field. Taking into account both the tree-level diagram and the diagrams with the self-energy insertions into the external legs (i.e. the tree-level diagram times $Z_M - 1$) yields a common factor Z_M which is equal to zero.

The diagram describing the meson mass function is shown in Fig. (1). The derivative of the mass function is calculated using the identity

$$\frac{d}{dp^2} = \frac{1}{2p^2} p^\mu \frac{d}{dp^\mu}. \quad (5)$$

In the case of the pseudoscalar and vector mesons the derivatives of the meson mass operator appearing in Eq. (4) are written as

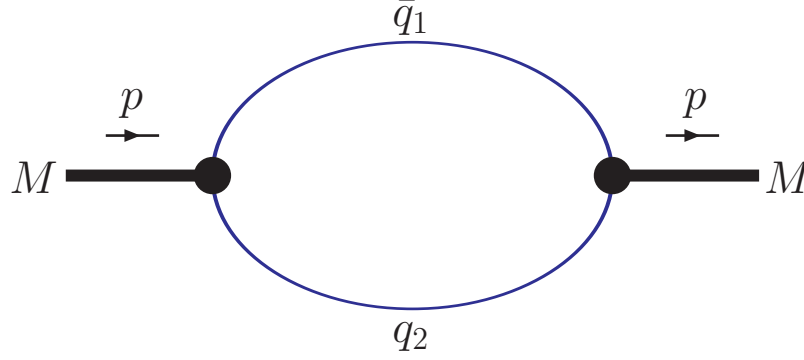


FIG. 1: Diagram describing the meson mass function.

$$\begin{aligned}
\tilde{\Pi}'_P(p^2) &= \frac{1}{2p^2} p^\alpha \frac{d}{dp^\alpha} \int \frac{d^4k}{4\pi^2 i} \tilde{\Phi}_P^2(-k^2) \text{tr} \left[\gamma^5 S_1(k + w_1 p) \gamma^5 S_2(k - w_2 p) \right] \\
&= \frac{1}{2p^2} \int \frac{d^4k}{4\pi^2 i} \tilde{\Phi}_P^2(-k^2) \left\{ w_1 \text{tr} \left[\gamma^5 S_1(k + w_1 p) \not{p} S_1(k + w_1 p) \gamma^5 S_2(k - w_2 p) \right] \right. \\
&\quad \left. - w_2 \text{tr} \left[\gamma^5 S_1(k + w_1 p) \gamma^5 S_2(k - w_2 p) \not{p} S_2(k - w_2 p) \right] \right\},
\end{aligned} \tag{6}$$

$$\begin{aligned}
\tilde{\Pi}'_V(p^2) &= \frac{1}{3} \left(g_{\mu\nu} - \frac{p_\mu p_\nu}{p^2} \right) \\
&\times \frac{1}{2p^2} p^\alpha \frac{d}{dp^\alpha} \int \frac{d^4k}{4\pi^2 i} \tilde{\Phi}_V^2(-k^2) \text{tr} \left[\gamma^\mu S_1(k + w_1 p) \gamma^\nu S_2(k - w_2 p) \right] \\
&= \frac{1}{3} \left(g_{\mu\nu} - \frac{p_\mu p_\nu}{p^2} \right) \\
&\times \frac{1}{2p^2} \int \frac{d^4k}{4\pi^2 i} \tilde{\Phi}_V^2(-k^2) \left\{ w_1 \text{tr} \left[\gamma^\mu S_1(k + w_1 p) \not{p} S_1(k + w_1 p) \gamma^\nu S_2(k - w_2 p) \right] \right. \\
&\quad \left. - w_2 \text{tr} \left[\gamma^\mu S_1(k + w_1 p) \gamma^\nu S_2(k - w_2 p) \not{p} S_2(k - w_2 p) \right] \right\},
\end{aligned} \tag{7}$$

where $\tilde{\Phi}_H(-k^2)$ is the Fourier-transform of the vertex function defined by Eq. (3). We use free fermion propagators for the quarks given by

$$S_i(k) = \frac{1}{m_{q_i} - \not{k}} \tag{8}$$

with an effective constituent quark mass m_{q_i} .

C. Infrared confinement

In the paper [50] we have included the confinement of quarks to our model. It was done, first, by introducing the scale integration in the space of α -parameters, and, second, by cutting this scale integration on the upper limit which corresponds to an infrared cutoff. In this manner one removes all possible thresholds present in the initial quark diagram. The cutoff parameter is taken to be the same for all physical processes. We have adjusted other model parameters by fitting the calculated quantities of the basic physical processes to available experimental data. In the papers [59, 60] we have applied the developed approach to the 4-body system - tetraquark X(3872).

Let us give the basic features of the infrared confinement in our model. All physical matrix elements are described by the Feynman diagrams which are the convolution of the free quark propagators and vertex functions. Let n , ℓ and m be the number of the propagators, loops and vertices, respectively. In the Minkowski space the ℓ -loop diagram will be represented as

$$\Pi(p_1, \dots, p_m) = \int [d^4 k]^\ell \prod_{i_1=1}^m \Phi_{i_1+n}(-K_{i_1+n}^2) \prod_{i_3=1}^n S_{i_3}(\tilde{k}_{i_3} + v_{i_3}),$$

$$K_{i_1+n}^2 = \sum_{i_2} (\tilde{k}_{i_1+n}^{(i_2)} + v_{i_1+n}^{(i_2)})^2, \quad (9)$$

where the vectors \tilde{k}_i are linear combinations of the loop momenta k_i . The v_i are linear combinations of the external momenta p_i to be specified in what follows. The strings of Dirac matrices appearing in the calculation need not concern us since they do not depend on the momenta. The external momenta p_i are all chosen to be ingoing such that one has $\sum_{i=1}^m p_i = 0$. All calculations proceed in the Euclidean region both for the loop momenta k_i and the external momenta p_i so that $k_i^2 \leq 0$, $p_i^2 \leq 0$.

Using the Schwinger representation of the local quark propagator one has

$$S(k) = (m + \not{k}) \int_0^\infty d\alpha e^{-\alpha(m^2 - k^2)}. \quad (10)$$

For the vertex functions one takes the Gaussian form

$$\Phi_{i+n}(-K^2) = \exp[\alpha_{i+n} K^2] \quad i = 1, \dots, m, \quad (11)$$

where the parameters $\alpha_{i+n} = s_i = 1/\Lambda_i^2$ are related to the size parameters. The integrand in Eq. (9) has a Gaussian form with the exponential $kak + 2kr + R$ where a is $\ell \times \ell$ matrix

depending on the parameter α_i , r is the ℓ -vector composed from the external momenta, and R is a quadratic form of the external momenta. Tensor loop integrals are calculated with the help of the differential representation

$$k_i^\mu e^{2kr} = \frac{1}{2} \frac{\partial}{\partial r_{i\mu}} e^{2kr}. \quad (12)$$

This allows to use the operator identity

$$\int d^4k P(k) e^{2kr} = \int d^4k P\left(\frac{1}{2} \frac{\partial}{\partial r}\right) e^{2kr} = P\left(\frac{1}{2} \frac{\partial}{\partial r}\right) \int d^4k e^{2kr} \quad (13)$$

which is written for one loop integration. The second identity then reads

$$\int_0^\infty d^n\alpha P\left(\frac{1}{2} \frac{\partial}{\partial r}\right) e^{-r^2/a} = \int_0^\infty d^n\alpha e^{-r^2/a} P\left(\frac{1}{2} \frac{\partial}{\partial r} - \frac{r}{a}\right), \quad (14)$$

where $r = r(\alpha_i)$ and $a = a(\Lambda_M, \alpha_i)$. It simplifies the computation following the trace evaluation: the polynomial in the derivative operator which results from the trace can be applied to an identity, instead being applied to a more complicated exponential function.

We have written a FORM [67] program that performs the necessary commutations of the differential operators in a very efficient way. After doing the loop integrations one obtains

$$\Pi = \int_0^\infty d^n\alpha F(\alpha_1, \dots, \alpha_n), \quad (15)$$

where F stands for the whole structure of a given diagram. The region over which the set of Schwinger parameters α_i is integrated can be turned into a simplex by introducing an additional t -integration via the identity

$$1 = \int_0^\infty dt \delta\left(t - \sum_{i=1}^n \alpha_i\right) \quad (16)$$

leading to

$$\Pi = \int_0^\infty dt t^{n-1} \int_0^1 d^n\alpha \delta\left(1 - \sum_{i=1}^n \alpha_i\right) F(t\alpha_1, \dots, t\alpha_n). \quad (17)$$

There are altogether n numerical integrations: $(n-1)$ α -parameter integrations and the integration over the scale parameter t . The very large t -region corresponds to the region where the singularities of the diagram with its local quark propagators start appearing. However, as described in [50], if one introduces an infrared cutoff on the upper limit of the

t -integration, all singularities vanish because the integral is now convergent for any value of the set of kinematic variables. We cut off the upper integration at $1/\lambda^2$ and obtain

$$\Pi^c = \int_0^{1/\lambda^2} dt t^{n-1} \int_0^1 d^n \alpha \delta\left(1 - \sum_{i=1}^n \alpha_i\right) F(t\alpha_1, \dots, t\alpha_n). \quad (18)$$

By introducing the infrared cutoff one has removed all potential thresholds in the quark loop diagram, i.e. the quarks are never on-shell and are thus effectively confined. Similar ideas have also been pursued in Refs. [68] where an infrared cutoff had been introduced in the context of a Nambu-Jona-Lasinio model by employing a proper time regularization. Such approach found some applications, in particular, for spectroscopy of charmonia [69]. Since the contact interaction has been employed one has to introduce also the ultraviolet cut-off. The values of both infrared and ultraviolet cut-off parameters are supposed to be different for different hadrons.

We take the infrared cutoff parameter λ to be the same in all physical processes. It may be understood from a proper time regularization of the generating functional describing the NJL model where a proper time is general for all matrix elements. Our “ t ”-integration parameter is analogous of a proper time and, hence, should not depend on the hadron characteristics of the certain process. It is important that we use nonlocal interactions of hadrons with their constituents. The relevant vertex functions characterize the properties of the hadron in such a way that the size parameters appearing in Eq. (3) are different for different hadrons. Their values are determined by fitting the calculated observables to the experimental data.

III. $B - K^*$ FORM FACTORS IN THE COVARIANT QUARK MODEL

Herein our primary subject is the matrix element which is described by the Feynman diagram shown in Fig. 2. It can be expressed via dimensionless form factors:

$$\begin{aligned}
& \langle V(p_2, \epsilon_2)_{[\bar{q}_1 q_3]} | \bar{q}_2 O^\mu q_1 | P_{[\bar{q}_3 q_2]}(p_1) \rangle = \\
& = N_c g_P g_V \int \frac{d^4 k}{(2\pi)^4 i} \tilde{\Phi}_P \left(-(k + w_{13} p_1)^2 \right) \tilde{\Phi}_V \left(-(k + w_{23} p_2)^2 \right) \\
& \times \text{tr} \left[O^\mu S_1(k + p_1) \gamma^5 S_3(k) \not{\epsilon}_2^\dagger S_2(k + p_2) \right] \\
& = \frac{\epsilon_\nu^\dagger}{m_1 + m_2} \left(-g^{\mu\nu} P \cdot q A_0(q^2) + P^\mu P^\nu A_+(q^2) + q^\mu P^\nu A_-(q^2) \right. \\
& \quad \left. + i \epsilon^{\mu\nu\alpha\beta} P_\alpha q_\beta V(q^2) \right), \tag{19}
\end{aligned}$$

$$\begin{aligned}
& \langle V(p_2, \epsilon_2)_{[\bar{q}_1 q_3]} | \bar{q}_2 (\sigma^{\mu\nu} q_\nu (1 + \gamma^5)) q_1 | P_{[\bar{q}_3 q_2]}(p_1) \rangle = \\
& = N_c g_P g_V \int \frac{d^4 k}{(2\pi)^4 i} \tilde{\Phi}_P \left(-(k + w_{13} p_1)^2 \right) \tilde{\Phi}_V \left(-(k + w_{23} p_2)^2 \right) \\
& \times \text{tr} \left[(\sigma^{\mu\nu} q_\nu (1 + \gamma^5)) S_1(k + p_1) \gamma^5 S_3(k) \not{\epsilon}_2^\dagger S_2(k + p_2) \right] \\
& = \epsilon_\nu^\dagger \left(- (g^{\mu\nu} - q^\mu q^\nu / q^2) P \cdot q a_0(q^2) + (P^\mu P^\nu - q^\mu P^\nu P \cdot q / q^2) a_+(q^2) \right. \\
& \quad \left. + i \epsilon^{\mu\nu\alpha\beta} P_\alpha q_\beta g(q^2) \right). \tag{20}
\end{aligned}$$

Here, $P = p_1 + p_2$, $q = p_1 - p_2$, $\epsilon_2^\dagger \cdot p_2 = 0$, $p_i^2 = m_i^2$. Since there are three sorts of quarks involved in these processes, we introduce the notation with two subscripts $w_{ij} = m_{q_j} / (m_{q_i} + m_{q_j})$ ($i, j = 1, 2, 3$) so that $w_{ij} + w_{ji} = 1$. The form factors defined in Eq. (20) satisfy the physical requirement $a_0(0) = a_+(0)$, which ensures that no kinematic singularity appears in the matrix element at $q^2 = 0$ GeV.

We will use the latest fit done in Ref. [70]. The fitted values of the constituent quark masses m_q , the infrared cutoff λ , and the size parameters Λ_H are given by Eq. (21) and Table I.

$m_{u/d}$	m_s	m_c	m_b	λ	
0.241	0.428	1.67	5.05	0.181	GeV

(21)

Our form factors are represented as three-fold integrals which are calculated by using NAG routines. They are shown in Figs. 3, 4 and 5. The results of our numerical calculations are

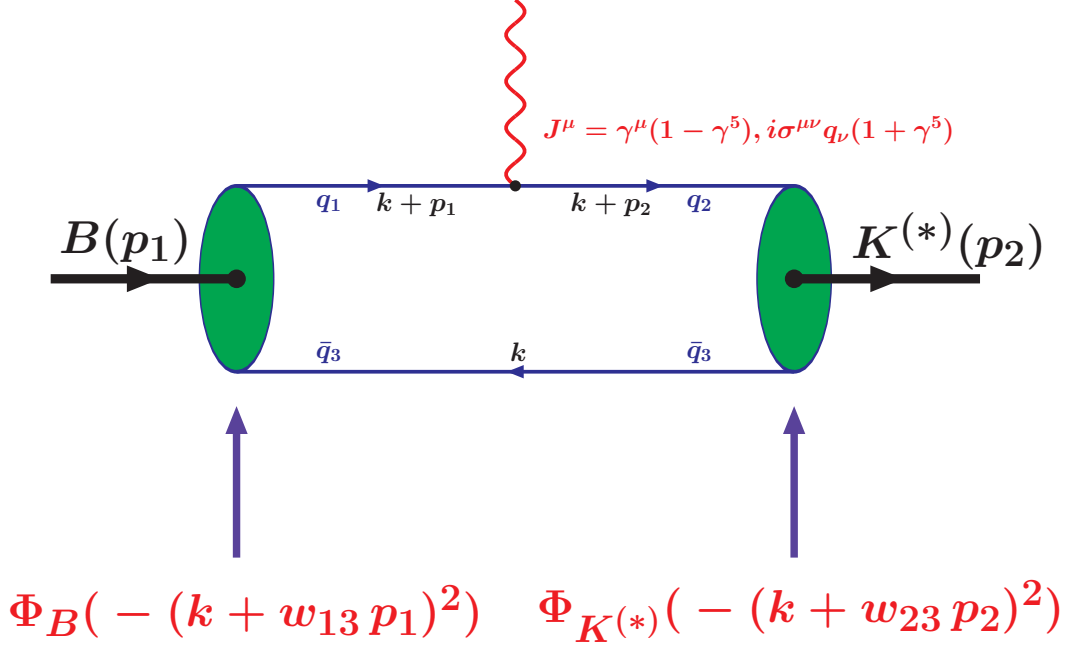


FIG. 2: Diagrammatic representation of the matrix elements describing $B \rightarrow K^*$ transitions.

TABLE I: The fitted values of the size parameters Λ_M in GeV.

π	K	D	D_s	B	B_s	B_c	η_c	η_b	
0.87	1.02	1.71	1.81	1.96	2.05	2.50	2.06	2.95	
ρ	ω	ϕ	J/ψ	K^*	D^*	D_s^*	B^*	B_s^*	Υ
0.61	0.50	0.91	1.93	0.75	1.51	1.71	1.76	1.71	2.96

well approximated by the parametrization

$$F(q^2) = \frac{F(0)}{1 - as + bs^2}, \quad s = \frac{q^2}{m_1^2}. \quad (22)$$

The values of $F(0)$, a , and b are listed in Table II. One can compare the obtained values of form factors at maximum recoil $q^2 = 0$ with those obtained in other approaches, see, for example, Table IV in [39] and references therein.

TABLE II: Parameters for the approximated form factors in Eqs. (22) of the $B \rightarrow K^*$ transitions.

	A_0	A_+	A_-	V	a_0	a_+	g
$F(0)$	0.459	0.310	-0.335	0.354	0.326	0.323	0.323
a	0.439	1.252	1.306	1.345	0.457	1.249	1.350
b	-0.311	0.270	0.316	0.343	-0.290	0.268	0.349

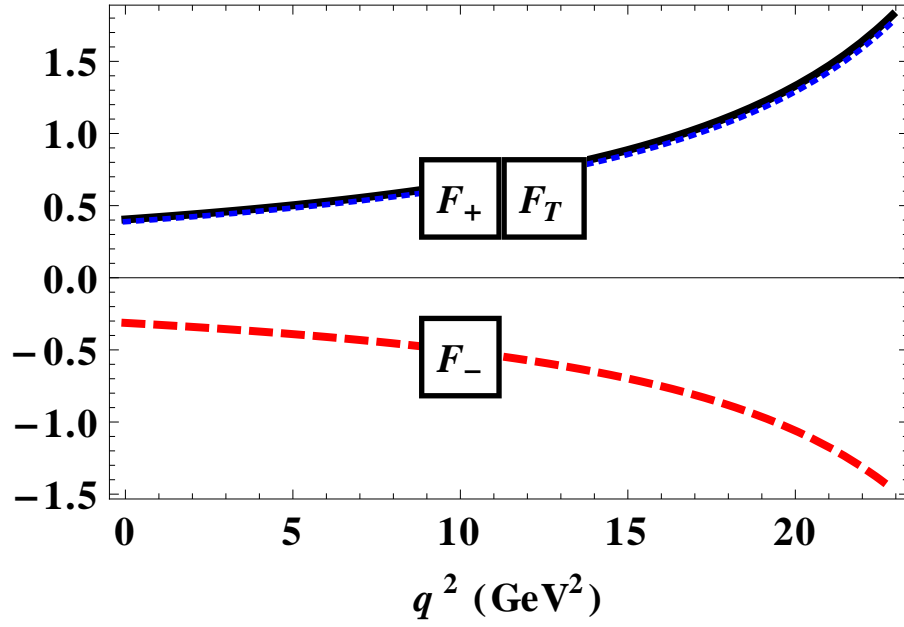


FIG. 3: The q^2 -dependence of the $B - K$ transition form factors.

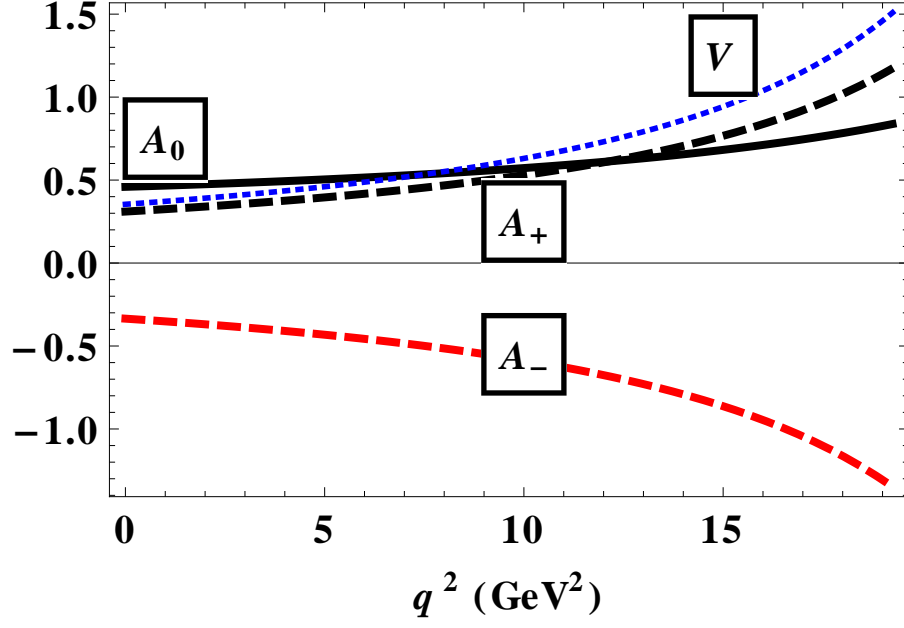


FIG. 4: The q^2 -dependence of the $B - K^*$ transition V, A form factors.

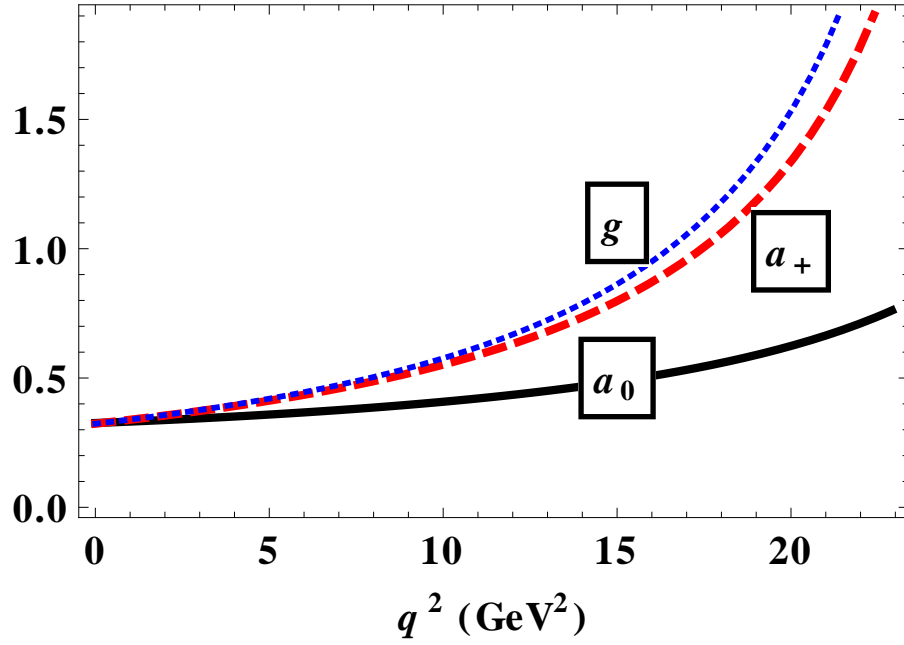


FIG. 5: The q^2 -dependence of the $B - K^*$ transition T form factors.

IV. EFFECTIVE HAMILTONIAN, INVARIANT AMPLITUDES AND DECAY DISTRIBUTIONS

The rare exclusive decays are described by the effective Hamiltonian obtained from the SM-diagrams using the operator product expansion and renormalization group techniques. It allows one to separate the short-distance contributions and isolate them in the Wilson coefficients which can be studied systematically within perturbative QCD. The long-distance contributions are contained in the matrix elements of local operators. Contrary to the short-distance contributions the calculation of such matrix elements requires nonperturbative methods and is therefore model dependent.

The rare decay $b \rightarrow s(d)\ell^+\ell^-$ can be described in terms of the effective Hamiltonian [71]:

$$\mathcal{H}_{\text{eff}} = -\frac{4G_F}{\sqrt{2}}\lambda_t \sum_{i=1}^{10} C_i(\mu)\mathcal{O}_i(\mu), \quad (23)$$

where $C_i(\mu)$ and $\mathcal{O}_i(\mu)$ are the Wilson coefficients and local operators, respectively. $\lambda_t \equiv |V_{ts}^*V_{tb}|$ is the product of CKM matrix elements. The standard set [71] of local operators for $b \rightarrow s\ell^+\ell^-$ transition is written as

$$\begin{aligned} \mathcal{O}_1 &= (\bar{s}_{a_1}\gamma^\mu P_L c_{a_2})(\bar{c}_{a_2}\gamma_\mu P_L b_{a_1}), \quad \mathcal{O}_2 = (\bar{s}\gamma^\mu P_L c)(\bar{c}\gamma_\mu P_L b), \\ \mathcal{O}_3 &= (\bar{s}\gamma^\mu P_L b) \sum_q (\bar{q}\gamma_\mu P_L q), \quad \mathcal{O}_4 = (\bar{s}_{a_1}\gamma^\mu P_L b_{a_2}) \sum_q (\bar{q}_{a_2}\gamma_\mu P_L q_{a_1}), \\ \mathcal{O}_5 &= (\bar{s}\gamma^\mu P_R b)_{V-A} \sum_q (\bar{q}\gamma_\mu P_R q), \quad \mathcal{O}_6 = (\bar{s}_{a_1}\gamma^\mu P_R b_{a_2}) \sum_q (\bar{q}_{a_2}\gamma_\mu P_R q_{a_1}), \\ \mathcal{O}_7 &= \frac{e}{16\pi^2}\bar{m}_b (\bar{s}\sigma^{\mu\nu} P_R b)F_{\mu\nu}, \quad \mathcal{O}_8 = \frac{g}{16\pi^2}\bar{m}_b (\bar{s}_{a_1}\sigma^{\mu\nu} P_R \mathbf{T}_{a_1 a_2} b_{a_2})\mathbf{G}_{\mu\nu}, \\ \mathcal{O}_9 &= \frac{e^2}{16\pi^2}(\bar{s}\gamma^\mu P_L b)(\bar{\ell}\gamma_\mu \ell), \quad \mathcal{O}_{10} = \frac{e^2}{16\pi^2}(\bar{s}\gamma^\mu P_L b)(\bar{\ell}\gamma_\mu \gamma_5 \ell), \end{aligned} \quad (24)$$

where $\mathbf{G}_{\mu\nu}$ and $F_{\mu\nu}$ are the gluon and photon field strengths, respectively; $\mathbf{T}_{a_1 a_2}$ are the generators of the $SU(3)$ color group; a_1 and a_2 denote color indices (they are omitted in the color-singlet currents). The chirality projection operators are $P_{L,R} = (1 \mp \gamma_5)/2$ and μ is a renormalization scale. $\mathcal{O}_{1,2}$ are current-current operators, \mathcal{O}_{3-6} are QCD penguin operators, $\mathcal{O}_{7,8}$ are "magnetic penguin" operators, and $\mathcal{O}_{9,10}$ are semileptonic electroweak penguin operators.

By using the effective Hamiltonian defined by Eq. (23) one can write the matrix element

of the exclusive transition $B \rightarrow K^* \ell^+ \ell^-$ as

$$\begin{aligned} \mathcal{M} = & \frac{G_F}{\sqrt{2}} \cdot \frac{\alpha \lambda_t}{\pi} \cdot \left\{ C_9^{\text{eff}} \langle K^* | \bar{s} \gamma^\mu P_L b | B \rangle (\bar{\ell} \gamma_\mu \ell) \right. \\ & - \frac{2\bar{m}_b}{q^2} C_7^{\text{eff}} \langle K^* | \bar{s} i \sigma^{\mu\nu} q_\nu P_R b | B \rangle (\bar{\ell} \gamma_\mu \ell) \\ & \left. + C_{10} \langle K^* | \bar{s} \gamma^\mu P_L b | B \rangle (\bar{\ell} \gamma_\mu \gamma_5 \ell) \right\}, \end{aligned} \quad (25)$$

where $C_7^{\text{eff}} = C_7 - C_5/3 - C_6$. One has to note that matrix element in Eq.(25) contains both a free quark decay amplitude coming from the operators \mathcal{O}_7 , \mathcal{O}_9 and \mathcal{O}_{10} (gluon magnetic penguin \mathcal{O}_8 does not contribute) and, in addition, certain long-distance effects from the matrix elements of four-quark operators \mathcal{O}_i ($i = 1, \dots, 6$) which usually are absorbed into a redefinition of the short-distance Wilson-coefficients. The Wilson coefficient C_9^{eff} effectively takes into account, first, the contributions from the four-quark operators \mathcal{O}_i ($i = 1, \dots, 6$) and, second, the nonperturbative effects coming from the $c\bar{c}$ -resonance contributions which are as usual parametrized by the Breit-Wigner ansatz [72]:

$$\begin{aligned} C_9^{\text{eff}} = & C_9 + C_0 \left\{ h(\hat{m}_c, s) + \frac{3\pi}{\alpha^2} \kappa \sum_{V_i=\psi(1s), \psi(2s)} \frac{\Gamma(V_i \rightarrow l^+ l^-) m_{V_i}}{m_{V_i}^2 - q^2 - i m_{V_i} \Gamma_{V_i}} \right\} \\ & - \frac{1}{2} h(1, s) (4C_3 + 4C_4 + 3C_5 + C_6) \\ & - \frac{1}{2} h(0, s) (C_3 + 3C_4) + \frac{2}{9} (3C_3 + C_4 + 3C_5 + C_6), \end{aligned} \quad (26)$$

where $C_0 \equiv 3C_1 + C_2 + 3C_3 + C_4 + 3C_5 + C_6$. Here the charm-loop function is written as

$$\begin{aligned} h(\hat{m}_c, s) = & -\frac{8}{9} \ln \frac{\bar{m}_b}{\mu} - \frac{8}{9} \ln \hat{m}_c + \frac{8}{27} + \frac{4}{9} x \\ & - \frac{2}{9} (2+x) |1-x|^{1/2} \begin{cases} \left(\ln \left| \frac{\sqrt{1-x}+1}{\sqrt{1-x}-1} \right| - i\pi \right), & \text{for } x \equiv \frac{4\hat{m}_c^2}{s} < 1, \\ 2 \arctan \frac{1}{\sqrt{x-1}}, & \text{for } x \equiv \frac{4\hat{m}_c^2}{s} > 1, \end{cases} \\ h(0, s) = & \frac{8}{27} - \frac{8}{9} \ln \frac{\bar{m}_b}{\mu} - \frac{4}{9} \ln s + \frac{4}{9} i\pi, \end{aligned}$$

where $\hat{m}_c = \bar{m}_c/m_B$, $s = q^2/m_B^2$ and $\kappa = 1/C_0$. In what follows we drop the charm resonance contributions by putting $\kappa = 0$. We denote the QCD quark masses by the bar symbol to distinguish them from the constituent quark masses used in the model, see Eq. (8). We will use the value of $\mu = \bar{m}_{b \text{ pole}}$ for the renormalization scale. The numerical values for the model-independent input parameters and the corresponding values of the Wilson coefficients are

given in Table IV. Besides the charm-loop perturbative contribution, two loop contributions have been calculated in [47]. A global analysis of $b \rightarrow s\ell\ell$ anomalies has been performed in Ref. [48] with the NNLL corrections included. It was shown that they amount up to 15%. The discussion of the non-local $c\bar{c}$ contributions maybe also found in Ref. [43].

We specify our choice of the momenta for the reaction $B(p_1) \rightarrow H_{\text{out}}(p_2) + \ell^+(k_1) + \ell^-(k_2)$ as $p_1 = p_2 + k_1 + k_2$ with $p_1^2 = m_1^2$, $p_2^2 = m_2^2$ and $k_1^2 = k_2^2 = m_\ell^2$ where k_1 and k_2 are the l^+ and l^- momenta, and m_1 , m_2 , m_ℓ are the masses of the initial B meson, final meson $H_{\text{out}} = K, K^*$ and lepton, respectively.

The matrix element in Eq (25) can now be written

$$\mathcal{M} = \frac{G_F}{\sqrt{2}} \cdot \frac{\alpha\lambda_t}{2\pi} \{T_1^\mu (\bar{\ell}\gamma_\mu\ell) + T_2^\mu (\bar{\ell}\gamma_\mu\gamma_5\ell)\}, \quad (27)$$

where the quantities T_i^μ are expressed through the form factors and the Wilson coefficients in the following manner:

$$T_i^\mu = T_i^{\mu\nu} \epsilon_{2\nu}^\dagger, \quad (i = 1, 2), \quad (28)$$

$$\begin{aligned} T_i^{\mu\nu} &= \frac{1}{m_1 + m_2} \left\{ -Pq g^{\mu\nu} A_0^{(i)} + P^\mu P^\nu A_+^{(i)} + q^\mu P^\nu A_-^{(i)} + i\varepsilon^{\mu\nu\alpha\beta} P_\alpha q_\beta V^{(i)} \right\}, \\ V^{(1)} &= C_9^{\text{eff}} V + C_7^{\text{eff}} g \frac{2\bar{m}_b(m_1 + m_2)}{q^2}, \\ A_0^{(1)} &= C_9^{\text{eff}} A_0 + C_7^{\text{eff}} a_0 \frac{2\bar{m}_b(m_1 + m_2)}{q^2}, \\ A_+^{(1)} &= C_9^{\text{eff}} A_+ + C_7^{\text{eff}} a_+ \frac{2\bar{m}_b(m_1 + m_2)}{q^2}, \\ A_-^{(1)} &= C_9^{\text{eff}} A_- + C_7^{\text{eff}} (a_0 - a_+) \frac{2\bar{m}_b(m_1 + m_2)}{q^2} \frac{Pq}{q^2}, \\ V^{(2)} &= C_{10} V, \quad A_0^{(2)} = C_{10} A_0, \quad A_\pm^{(2)} = C_{10} A_\pm. \end{aligned} \quad (29)$$

Let us consider the decay distribution differential in the momentum transfer squared q^2 and in the polar angle. The latter is defined as the angle between $\vec{q} = \vec{p}_1 - \vec{p}_2$ and \vec{k}_1 ($\ell^+\ell^-$ rest frame) as shown in Fig. 6. By using the notation from Ref. [49] and correcting some

obvious typos, one has

$$\begin{aligned}
\frac{d^2\Gamma}{dq^2 d\cos\theta} &= \frac{|\mathbf{p}_2| \beta_\ell}{(2\pi)^3 4 m_1^2} \cdot \frac{1}{8} \sum_{\text{pol}} |M|^2 = \frac{G_F^2}{(2\pi)^3} \left(\frac{\alpha |\lambda_t|}{2\pi} \right)^2 \frac{|\mathbf{p}_2| \beta_\ell}{8 m_1^2} \\
&\times \frac{1}{8} \left\{ H_{11}^{\mu\nu} \cdot \text{tr}[\gamma_\mu (\not{k}_1 - m_\ell) \gamma_\nu (\not{k}_2 + m_\ell)] \right. \\
&+ H_{22}^{\mu\nu} \cdot \text{tr}[\gamma_\mu \gamma_5 (\not{k}_1 - m_\ell) \gamma_\nu \gamma_5 (\not{k}_2 + m_\ell)] \\
&- H_{12}^{\mu\nu} \cdot \text{tr}[\gamma_\mu (\not{k}_1 - m_\ell) \gamma_\nu \gamma_5 (\not{k}_2 + m_\ell)] \\
&\left. - H_{21}^{\mu\nu} \cdot \text{tr}[\gamma_\mu \gamma_5 (\not{k}_1 - m_\ell) \gamma_\nu (\not{k}_2 + m_\ell)] \right\} \\
&= \frac{G_F^2}{(2\pi)^3} \left(\frac{\alpha |\lambda_t|}{2\pi} \right)^2 \frac{|\mathbf{p}_2| \beta_\ell}{8 m_1^2} \cdot \frac{1}{2} \left\{ L_{\mu\nu}^{(1)} \cdot (H_{11}^{\mu\nu} + H_{22}^{\mu\nu}) \right. \\
&\left. - \frac{1}{2} L_{\mu\nu}^{(2)} \cdot (q^2 H_{11}^{\mu\nu} + (q^2 - 4m_\ell^2) H_{22}^{\mu\nu}) + L_{\mu\nu}^{(3)} \cdot (H_{12}^{\mu\nu} + H_{21}^{\mu\nu}) \right\},
\end{aligned} \tag{30}$$

where $|\mathbf{p}_2| = \lambda^{1/2}(m_1^2, m_2^2, q^2)/2m_1$ is the momentum of the K^* -meson given in the B -rest frame and $\beta_\ell = \sqrt{1 - 4m_\ell^2/q^2}$. We have introduced lepton and hadron tensors as

$$L_{\mu\nu}^{(1)} = k_{1\mu} k_{2\nu} + k_{2\mu} k_{1\nu}, \quad L_{\mu\nu}^{(2)} = g_{\mu\nu}, \quad L_{\mu\nu}^{(3)} = i \varepsilon_{\mu\nu\alpha\beta} k_1^\alpha k_2^\beta, \tag{31}$$

$$H_{ij}^{\mu\nu} = T_i^\mu T_j^{\dagger\nu}. \tag{32}$$

We use the following convention for the γ_5 -matrix and the Levy-Civita tensor in Minkowski space:

$$\gamma^0 = \begin{pmatrix} I & 0 \\ 0 & -I \end{pmatrix}, \quad \gamma^k = \begin{pmatrix} 0 & \sigma_k \\ -\sigma_k & 0 \end{pmatrix}, \quad \gamma^5 = \gamma_5 = i \gamma^0 \gamma^1 \gamma^2 \gamma^3 = \begin{pmatrix} 0 & I \\ I & 0 \end{pmatrix}, \tag{33}$$

$$\text{tr}(\gamma_5 \gamma^\mu \gamma^\nu \gamma^\alpha \gamma^\beta) = 4 i \varepsilon^{\mu\nu\alpha\beta}, \quad \text{tr}(\gamma_5 \gamma_\mu \gamma_\nu \gamma_\alpha \gamma_\beta) = 4 i \varepsilon_{\mu\nu\alpha\beta}, \quad \varepsilon_{0123} = -\varepsilon^{0123} = +1.$$

The Lorentz contractions in Eq. (30) can be evaluated in terms of helicity amplitudes as described in [22, 49]. First, we define an orthonormal and complete helicity basis $\epsilon^\mu(m)$ with the three spin 1 components orthogonal to the momentum transfer q^μ , i.e. $\epsilon^\mu(m) q_\mu = 0$ for $m = \pm, 0$, and the spin 0 (time)-component $m = t$ with $\epsilon^\mu(t) = q^\mu / \sqrt{q^2}$. The orthonormality and completeness properties read

$$\epsilon_\mu^\dagger(m) \epsilon^\mu(n) = g_{mn}, \quad (m, n = t, \pm, 0), \quad \text{orthonormality},$$

$$\epsilon_\mu(m) \epsilon_\nu^\dagger(n) g_{mn} = g_{\mu\nu}, \quad \text{completeness}, \tag{34}$$

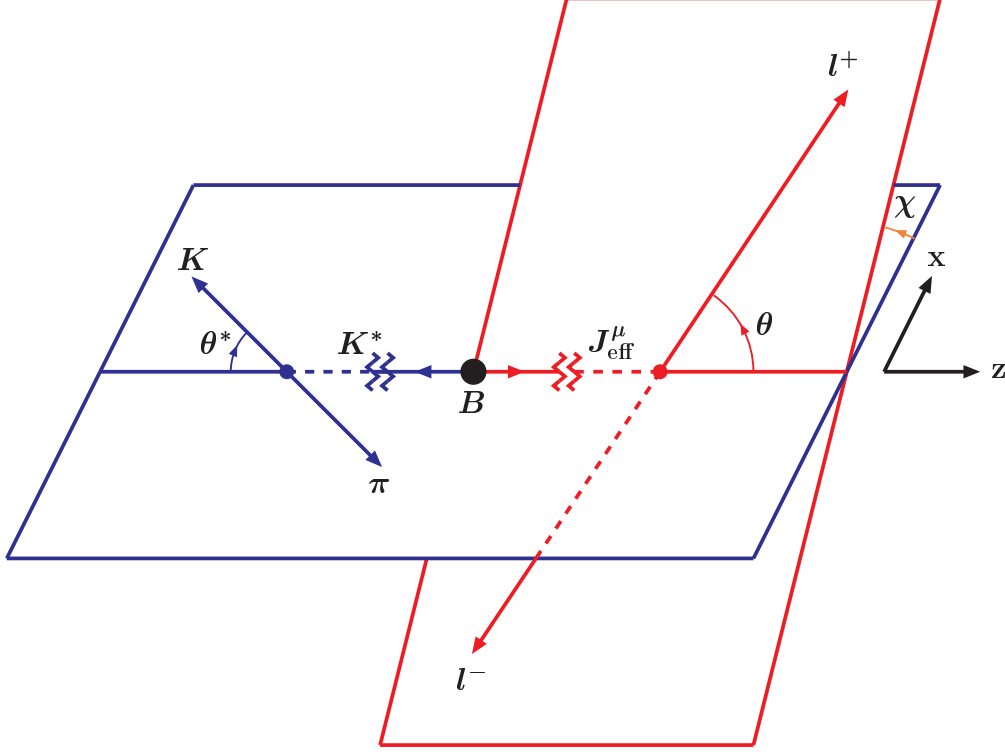


FIG. 6: Definition of the angles θ , θ^* and χ in the cascade decay $B \rightarrow K^*(\rightarrow K\pi)\bar{\ell}\ell$.

with $g_{mn} = \text{diag}(+, -, -, -)$. We include the time component polarization vector $\epsilon^\mu(t)$ in the set because we want to discuss lepton mass effects.

Using the completeness property one can rewrite the contraction of the lepton and hadron tensors in Eq. (30) as follows

$$\begin{aligned} L^{(k)\mu\nu} H_{\mu\nu}^{ij} &= L_{\mu'\nu'}^{(k)} \epsilon^{\mu'}(m) \epsilon^{\dagger\mu}(m') g_{mm'} \epsilon^{\dagger\nu'}(n) \epsilon^\nu(n') g_{nn'} H_{\mu\nu}^{ij} \\ &= L_{mn}^{(k)} g_{mm'} g_{nn'} H_{m'n'}^{ij}, \end{aligned} \quad (35)$$

where we have introduced the lepton and hadron tensors in the space of the helicity components

$$L_{mn}^{(k)} = \epsilon^\mu(m) \epsilon^{\dagger\nu}(n) L_{\mu\nu}^{(k)}, \quad H_{mn}^{ij} = \epsilon^{\dagger\mu}(m) \epsilon^\nu(n) H_{\mu\nu}^{ij}. \quad (36)$$

The two tensors can be evaluated in two different Lorentz systems. The lepton tensors $L_{mn}^{(k)}$ will be evaluated in the $\bar{\ell}\ell$ -CM system whereas the hadron tensors H_{mn}^{ij} will be evaluated in the B rest system.

In the B rest frame the momenta and polarization vectors can be written as

$$\begin{aligned} p_1^\mu &= (m_1, 0, 0, 0), & \epsilon^\mu(t) &= \frac{1}{\sqrt{q^2}}(q_0, 0, 0, |\mathbf{p}_2|), \\ p_2^\mu &= (E_2, 0, 0, -|\mathbf{p}_2|), & \epsilon^\mu(\pm) &= \frac{1}{\sqrt{2}}(0, \mp 1, -i, 0), \\ q^\mu &= (q_0, 0, 0, +|\mathbf{p}_2|), & \epsilon^\mu(0) &= \frac{1}{\sqrt{q^2}}(|\mathbf{p}_2|, 0, 0, q_0), \end{aligned}$$

where $E_2 = (m_1^2 + m_2^2 - q^2)/2m_1$ and $q_0 = (m_1^2 - m_2^2 + q^2)/2m_1$. Using this basis one can express the components of the hadronic tensors through the invariant form factors defined in Eqs. (19) and (20). One has

$$\begin{aligned} H_{mn}^{ij} &= \epsilon^{\dagger\mu}(m)\epsilon^\nu(n)H_{\mu\nu}^{ij} = \epsilon^{\dagger\mu}(m)\epsilon^\nu(n)T_{\mu\alpha}^i \left(-g^{\alpha\beta} + \frac{p_2^\alpha p_2^\beta}{m_2^2} \right) T_{\beta\nu}^{\dagger j} \\ &= \epsilon^{\dagger\mu}(m)\epsilon^\nu(n)T_{\mu\alpha}^i \epsilon_2^{\dagger\alpha}(r)\epsilon_2^\beta(s)\delta_{rs}T_{\beta\nu}^{\dagger j} \\ &= \epsilon^{\dagger\mu}(m)\epsilon_2^{\dagger\alpha}(r)T_{\mu\alpha}^i \cdot \left(\epsilon^{\dagger\nu}(n)\epsilon_2^{\dagger\beta}(s)T_{\nu\beta}^j \right)^\dagger \delta_{rs} \equiv H_m^i H_n^{\dagger j}. \end{aligned} \quad (37)$$

From angular momentum conservation one has $r = m$ and $s = n$ for $m, n = \pm, 0$ and $r, s = 0$ for $m, n = t$. The helicity components $\epsilon_2(m)$ ($m = \pm, 0$) of the polarization vector of the K^* read

$$\epsilon_2^\mu(\pm) = \frac{1}{\sqrt{2}}(0, \pm 1, -i, 0), \quad \epsilon_2^\mu(0) = \frac{1}{m_2}(|\mathbf{p}_2|, 0, 0, -E_2). \quad (38)$$

Then one obtains the non-zero components of the hadron tensors

$$\begin{aligned} H_{t0}^i &= \epsilon^{\dagger\mu}(t)\epsilon_2^{\dagger\alpha}(0)T_{\mu\alpha}^i = \frac{1}{m_1 + m_2} \frac{m_1 |\mathbf{p}_2|}{m_2 \sqrt{q^2}} (Pq(-A_0^i + A_+^i) + q^2 A_-^i), \\ H_{\pm 1 \pm 1}^i &= \epsilon^{\dagger\mu}(\pm)\epsilon_2^{\dagger\alpha}(\pm)T_{\mu\alpha}^i = \frac{1}{m_1 + m_2} (-Pq A_0^i \pm 2m_1 |\mathbf{p}_2| V^i), \\ H_{00}^i &= \epsilon^{\dagger\mu}(0)\epsilon_2^{\dagger\alpha}(0)T_{\mu\alpha}^i = \\ &= \frac{1}{m_1 + m_2} \frac{1}{2m_2 \sqrt{q^2}} (-Pq(m_1^2 - m_2^2 - q^2) A_0^i + 4m_1^2 |\mathbf{p}_2|^2 A_+^i). \end{aligned} \quad (39)$$

The lepton tensors $L_{mn}^{(k)}$ are evaluated in the $\bar{\ell}\ell$ -CM system $\vec{k}_1 + \vec{k}_2 = 0$.

$$\begin{aligned} q^\mu &= (\sqrt{q^2}, 0, 0, 0), & k_1^\mu &= (E_1, +|\mathbf{k}_1| \sin \theta, 0, +|\mathbf{k}_1| \cos \theta), \\ & & k_2^\mu &= (E_1, -|\mathbf{k}_1| \sin \theta, 0, -|\mathbf{k}_1| \cos \theta), \end{aligned}$$

with $E_1 = \sqrt{q^2}/2$ and $|\mathbf{k}_1| = \sqrt{q^2 - 4m_\ell^2}/2$. The longitudinal and time component of polarization vectors in the $\bar{\ell}\ell$ rest frame are given by

$$\epsilon(t) = (1, 0, 0, 0), \quad \epsilon^\mu(\pm) = \frac{1}{\sqrt{2}}(0, \mp 1, -i, 0), \quad \epsilon^\mu(0) = (0, 0, 0, 1).$$

The differential $(q^2, \cos\theta)$ distribution finally reads

$$\begin{aligned} \frac{d\Gamma(B \rightarrow K^* \bar{\ell}\ell)}{dq^2 d\cos\theta} &= \frac{G_F^2}{(2\pi)^3} \left(\frac{\alpha|\lambda_t|}{2\pi} \right)^2 \frac{|\mathbf{p}_2| q^2 \beta_\ell}{32 m_1^2} \\ &\times \left\{ (1 + \cos^2\theta) \cdot \frac{1}{2} (\mathcal{H}_U^{11} + \mathcal{H}_U^{22}) + \sin^2\theta (\mathcal{H}_L^{11} + \mathcal{H}_L^{22}) - 2\beta_\ell \cos\theta \cdot \mathcal{H}_P^{12} \right. \\ &+ \delta_{\ell\ell} [\sin^2\theta \cdot \mathcal{H}_U^{11} - (1 + \cos^2\theta) \cdot \mathcal{H}_U^{22} \\ &\left. + 2\cos^2\theta \cdot \mathcal{H}_L^{11} - 2\sin^2\theta \cdot \mathcal{H}_L^{22} + 2\mathcal{H}_S^{22}] \right\}, \end{aligned} \quad (40)$$

where the helicity flip suppression factor $\delta_{\ell\ell}$ is given by

$$\delta_{\ell\ell} = \frac{2m_\ell^2}{q^2}.$$

After integrating over $\cos\theta$ one obtains

$$\begin{aligned} \frac{d\Gamma(B \rightarrow K^* \bar{\ell}\ell)}{dq^2} &= \frac{G_F^2}{(2\pi)^3} \left(\frac{\alpha|\lambda_t|}{2\pi} \right)^2 \frac{|\mathbf{p}_2| q^2 \beta_\ell}{12 m_1^2} \mathcal{H}_{\text{tot}}, \\ \mathcal{H}_{\text{tot}} &= \frac{1}{2} (\mathcal{H}_U^{11} + \mathcal{H}_U^{22} + \mathcal{H}_L^{11} + \mathcal{H}_L^{22}) + \delta_{\ell\ell} \left[\frac{1}{2} \mathcal{H}_U^{11} - \mathcal{H}_U^{22} + \frac{1}{2} \mathcal{H}_L^{11} - \mathcal{H}_L^{22} + \frac{3}{2} \mathcal{H}_S^{22} \right]. \end{aligned} \quad (41)$$

The relevant bilinear combinations of the helicity amplitudes are defined in Table III. Note that we drop a factor of “3” in the notation of \mathcal{H}_S and \mathcal{H}_{IS} compared with our paper [49].

V. FOUR-FOLD DISTRIBUTION IN CASCADE DECAY $B \rightarrow K^*(\rightarrow K\pi)\bar{\ell}\ell$

The lepton-hadron correlation function $L_{\mu\nu} H^{\mu\nu}$ reveals even more structure when one uses the cascade decay $B \rightarrow K^*(\rightarrow K\pi)\bar{\ell}\ell$ to analyze the polarization of the K^* . The hadron tensor now reads [49]

$$H_{\mu\nu}^{ij} = T_{\mu\alpha}^i (T_{\nu\beta}^j)^\dagger \frac{3}{2|\mathbf{p}_3|} \text{Br}(K^* \rightarrow K\pi) p_{3\alpha} p_{3\beta} S^{\alpha\alpha'}(p_2) S^{\beta\beta'}(p_2), \quad (42)$$

where $S^{\alpha\alpha'}(p_2) = -g^{\alpha\alpha'} + p_2^\alpha p_2^{\alpha'}/m_2^2$ is the standard spin 1 tensor, $p_2 = p_3 + p_4$, $p_3^2 = m_K^2$, $p_4^2 = m_\pi^2$, and p_3 and p_4 are the momenta of the K and the π , respectively. The relative configuration of the (K, π) - and $(\bar{\ell}\ell)$ -planes is shown in Fig. 6. The branching ratio $\text{Br}(K^* \rightarrow K\pi) \approx 1$ so we drop it off in what follows.

In the rest frame of the K^* one has

$$\begin{aligned}
p_2^\mu &= (m_2, \vec{0}), \\
p_3^\mu &= (E_3, +|\mathbf{p}_3| \sin \theta^*, 0, -|\mathbf{p}_3| \cos \theta^*), \\
p_4^\mu &= (E_4, -|\mathbf{p}_3| \sin \theta^*, 0, +|\mathbf{p}_3| \cos \theta^*),
\end{aligned} \tag{43}$$

where $|\mathbf{p}_3| = \lambda^{1/2}(m_2^2, m_3^2, m_4^2)/(2m_2)$. According to Eq. (38) the rest frame polarization vectors of the K^* are given by

$$\epsilon_2^\mu(\pm) = \frac{1}{\sqrt{2}}(0, \pm 1, -i, 0), \quad \epsilon_2^\mu(0) = (0, 0, 0, -1). \tag{44}$$

The spin 1 tensor $S^{\alpha\alpha'}(p_2)$ is then written as

$$S^{\alpha\alpha'}(p_2) = -g^{\alpha\alpha'} + \frac{p_2^\alpha p_2^{\alpha'}}{m_2^2} = \sum_{m=\pm,0} \epsilon_2^\alpha(m) \epsilon_2^{\dagger\alpha'}(m). \tag{45}$$

TABLE III: Definition of helicity structure functions and their parity properties.

parity-conserving (p.c.)	parity-violating (p.v.)
$\mathcal{H}_U^{ij} = \text{Re} \left(H_{+1+1}^i H_{+1+1}^{\dagger j} \right) + \text{Re} \left(H_{-1-1}^i H_{-1-1}^{\dagger j} \right)$	$\mathcal{H}_P^{ij} = \text{Re} \left(H_{+1+1}^i H_{+1+1}^{\dagger j} \right) - \text{Re} \left(H_{-1-1}^i H_{-1-1}^{\dagger j} \right)$
$\mathcal{H}_{IU}^{ij} = \text{Im} \left(H_{+1+1}^i H_{+1+1}^{\dagger j} \right) + \text{Im} \left(H_{-1-1}^i H_{-1-1}^{\dagger j} \right)$	$\mathcal{H}_{IP}^{ij} = \text{Im} \left(H_{+1+1}^i H_{+1+1}^{\dagger j} \right) - \text{Im} \left(H_{-1-1}^i H_{-1-1}^{\dagger j} \right)$
$\mathcal{H}_L^{ij} = \text{Re} \left(H_{00}^i H_{00}^{\dagger j} \right)$	$\mathcal{H}_A^{ij} = \frac{1}{2} \left[\text{Re} \left(H_{+1+1}^i H_{00}^{\dagger j} \right) - \text{Re} \left(H_{-1-1}^i H_{00}^{\dagger j} \right) \right]$
$\mathcal{H}_{IL}^{ij} = \text{Im} \left(H_{00}^i H_{00}^{\dagger j} \right)$	$\mathcal{H}_{IA}^{ij} = \frac{1}{2} \left[\text{Im} \left(H_{+1+1}^i H_{00}^{\dagger j} \right) - \text{Im} \left(H_{-1-1}^i H_{00}^{\dagger j} \right) \right]$
$\mathcal{H}_T^{ij} = \text{Re} \left(H_{+1+1}^i H_{-1-1}^{\dagger j} \right)$	$\mathcal{H}_{SA}^{ij} = \frac{1}{2} \left[\text{Re} \left(H_{+1+1}^i H_{0t}^{\dagger j} \right) - \text{Re} \left(H_{-1-1}^i H_{0t}^{\dagger j} \right) \right]$
$\mathcal{H}_{IT}^{ij} = \text{Im} \left(H_{+1+1}^i H_{-1-1}^{\dagger j} \right)$	$\mathcal{H}_{ISA}^{ij} = \frac{1}{2} \left[\text{Im} \left(H_{+1+1}^i H_{0t}^{\dagger j} \right) - \text{Im} \left(H_{-1-1}^i H_{0t}^{\dagger j} \right) \right]$
$\mathcal{H}_I^{ij} = \frac{1}{2} \left[\text{Re} \left(H_{+1+1}^i H_{00}^{\dagger j} \right) + \text{Re} \left(H_{-1-1}^i H_{00}^{\dagger j} \right) \right]$	
$\mathcal{H}_{II}^{ij} = \frac{1}{2} \left[\text{Im} \left(H_{+1+1}^i H_{00}^{\dagger j} \right) + \text{Im} \left(H_{-1-1}^i H_{00}^{\dagger j} \right) \right]$	
$\mathcal{H}_S^{ij} = \text{Re} \left(H_{0t}^i H_{0t}^{\dagger j} \right)$	
$\mathcal{H}_{IS}^{ij} = \text{Im} \left(H_{0t}^i H_{0t}^{\dagger j} \right)$	
$\mathcal{H}_{ST}^{ij} = \frac{1}{2} \left[\text{Re} \left(H_{+1+1}^i H_{0t}^{\dagger j} \right) + \text{Re} \left(H_{-1-1}^i H_{0t}^{\dagger j} \right) \right]$	
$\mathcal{H}_{IST}^{ij} = \frac{1}{2} \left[\text{Im} \left(H_{+1+1}^i H_{0t}^{\dagger j} \right) + \text{Im} \left(H_{-1-1}^i H_{0t}^{\dagger j} \right) \right]$	
$\mathcal{H}_{SL}^{ij} = \text{Re} \left(H_{00}^i H_{0t}^{\dagger j} \right)$	
$\mathcal{H}_{ISL}^{ij} = \text{Im} \left(H_{00}^i H_{0t}^{\dagger j} \right)$	

Following basically the same trick as in Eq. (35) the contraction of the lepton and hadron tensors may be written through helicity components. Finally, one obtains the full four-fold angular decay distribution

$$\begin{aligned}
\frac{d\Gamma(B \rightarrow K^*(\rightarrow K\pi)\bar{\ell}\ell)}{dq^2 d\cos\theta d(\chi/2\pi) d\cos\theta^*} &= \frac{G_F^2}{(2\pi)^3} \left(\frac{\alpha|\lambda_t|}{2\pi} \right)^2 \frac{|\mathbf{p}_2| q^2 \beta_\ell}{12 m_1^2} W(\theta^*, \theta, \chi), \\
W(\theta^*, \theta, \chi) &= \frac{9}{64} (1 + \cos^2 \theta) \sin^2 \theta^* (\mathcal{H}_U^{11} + \mathcal{H}_U^{22}) + \frac{9}{16} \sin^2 \theta \cos^2 \theta^* (\mathcal{H}_L^{11} + \mathcal{H}_L^{22}) \\
&- \frac{9}{32} \sin^2 \theta \sin^2 \theta^* \cos 2\chi (\mathcal{H}_T^{11} + \mathcal{H}_T^{22}) + \frac{9}{32} \sin 2\theta \sin 2\theta^* \cos \chi (\mathcal{H}_I^{11} + \mathcal{H}_I^{22}) \\
&+ \beta_\ell \left[-\frac{9}{16} \cos \theta \sin^2 \theta^* \mathcal{H}_P^{12} \right. \\
&\quad \left. - \frac{9}{16} \sin \theta \sin 2\theta^* \cos \chi (\mathcal{H}_A^{12} + \mathcal{H}_A^{21}) + \frac{9}{16} \sin \theta \sin 2\theta^* \sin \chi (\mathcal{H}_{II}^{12} + \mathcal{H}_{II}^{21}) \right] \\
&- \frac{9}{32} \sin 2\theta \sin 2\theta^* \sin \chi (\mathcal{H}_{IA}^{11} + \mathcal{H}_{IA}^{22}) + \frac{9}{32} \sin^2 \theta \sin^2 \theta^* \sin 2\chi (\mathcal{H}_{IT}^{11} + \mathcal{H}_{IT}^{22}) \\
&+ \delta_{\ell\ell} \left\{ \frac{9}{32} \sin^2 \theta \sin^2 \theta^* \mathcal{H}_U^{11} - \frac{9}{32} (1 + \cos^2 \theta) \sin^2 \theta^* \mathcal{H}_U^{22} \right. \\
&\quad + \frac{9}{8} \cos^2 \theta \cos^2 \theta^* \mathcal{H}_L^{11} - \frac{9}{8} \sin^2 \theta \cos^2 \theta^* \mathcal{H}_L^{22} \\
&\quad + \frac{9}{16} \sin^2 \theta \sin^2 \theta^* \cos 2\chi (\mathcal{H}_T^{11} + \mathcal{H}_T^{22}) \\
&\quad - \frac{9}{16} \sin 2\theta \sin 2\theta^* \cos \chi (\mathcal{H}_I^{11} + \mathcal{H}_I^{22}) + \frac{9}{8} \cos^2 \theta^* \mathcal{H}_S^{22} \\
&\quad + \frac{9}{16} \sin 2\theta \sin 2\theta^* \sin \chi (\mathcal{H}_{IA}^{11} + \mathcal{H}_{IA}^{22}) \\
&\quad \left. - \frac{9}{16} \sin^2 \theta \sin^2 \theta^* \sin 2\chi (\mathcal{H}_{IT}^{11} + \mathcal{H}_{IT}^{22}) \right\}. \tag{46}
\end{aligned}$$

The differential angular decay distribution in the Ref. ([26]) is expressed via the transversality amplitudes A_\perp , A_\parallel , A_0 and A_t . They are related to our helicity amplitudes as

$$\begin{aligned}
A_\perp^{L,R} &= N \frac{1}{\sqrt{2}} \left[(H_{+1+1}^{(1)} - H_{-1-1}^{(1)}) \mp (H_{+1+1}^{(2)} - H_{-1-1}^{(2)}) \right], \\
A_\parallel^{L,R} &= N \frac{1}{\sqrt{2}} \left[(H_{+1+1}^{(1)} + H_{-1-1}^{(1)}) \mp (H_{+1+1}^{(2)} + H_{-1-1}^{(2)}) \right], \\
A_0^{L,R} &= N \left(H_{00}^{(1)} \mp H_{00}^{(2)} \right), \\
A_t &= -2 N H_{0t}^{(2)}, \tag{47}
\end{aligned}$$

where the overall factor is given by

$$N = \left[\frac{1}{4} \frac{G_F^2}{(2\pi)^3} \left(\frac{\alpha|\lambda_t|}{2\pi} \right)^2 \frac{|\mathbf{p}_2| q^2 \beta_\ell}{12 m_1^2} \right]^{\frac{1}{2}}.$$

One can check that the four-fold angular distribution in Eq.(46) agrees with those obtained in [26] Eq.(3.1).

The four-body distribution of the cascade decay $B_d^0 \rightarrow K^{*0}(\rightarrow K\pi)\ell^+\ell^-$ is now often written in the form as given in Ref. [28]

$$\begin{aligned} \frac{d^4\Gamma}{dq^2 d\cos\theta^* d\cos\theta d\chi} = & \frac{9}{32\pi} \left[J_{1s} \sin^2\theta^* + J_{1c} \cos^2\theta^* + (J_{2s} \sin^2\theta^* + J_{2c} \cos^2\theta^*) \cos 2\theta \right. \\ & + J_3 \sin^2\theta^* \sin^2\theta \cos 2\chi + J_4 \sin 2\theta^* \sin 2\theta \cos \chi + J_5 \sin 2\theta^* \sin \theta \cos \chi \\ & + (J_{6s} \sin^2\theta^* + J_{6c} \cos^2\theta^*) \cos \theta + J_7 \sin 2\theta^* \sin \theta \sin \chi + J_8 \sin 2\theta^* \sin 2\theta \sin \chi \\ & \left. + J_9 \sin^2\theta^* \sin^2\theta \sin 2\chi \right], \end{aligned} \quad (48)$$

where the expressions for the coefficients J_i are written as

$$\begin{aligned} J_{1s} &= \frac{(2 + \beta_\ell^2)}{4} [|A_\perp^L|^2 + |A_\parallel^L|^2 + |A_\perp^R|^2 + |A_\parallel^R|^2] + \frac{4m_\ell^2}{q^2} \text{Re}(A_\perp^L A_\perp^{R*} + A_\parallel^L A_\parallel^{R*}), \\ J_{1c} &= |A_0^L|^2 + |A_0^R|^2 + \frac{4m_\ell^2}{q^2} [|A_t|^2 + 2\text{Re}(A_0^L A_0^{R*})] + \beta_\ell^2 |A_S|^2, \\ J_{2s} &= \frac{\beta_\ell^2}{4} [|A_\perp^L|^2 + |A_\parallel^L|^2 + |A_\perp^R|^2 + |A_\parallel^R|^2], \quad J_{2c} = -\beta_\ell^2 [|A_0^L|^2 + |A_0^R|^2], \\ J_3 &= \frac{1}{2}\beta_\ell^2 [|A_\perp^L|^2 - |A_\parallel^L|^2 + |A_\perp^R|^2 - |A_\parallel^R|^2], \quad J_4 = \frac{1}{\sqrt{2}}\beta_\ell^2 [\text{Re}(A_0^L A_\parallel^{L*} + A_0^R A_\parallel^{R*})], \\ J_5 &= \sqrt{2}\beta_\ell \left[\text{Re}(A_0^L A_\perp^{L*} - A_0^R A_\perp^{R*}) - \frac{m_\ell}{\sqrt{q^2}} \text{Re}(A_\parallel^L A_S^* + A_\parallel^{R*} A_S) \right], \\ J_{6s} &= 2\beta_\ell [\text{Re}(A_\parallel^L A_\perp^{L*} - A_\parallel^R A_\perp^{R*})], \quad J_{6c} = 4\beta_\ell \frac{m_\ell}{\sqrt{q^2}} \text{Re}(A_0^L A_S^* + A_0^{R*} A_S), \\ J_7 &= \sqrt{2}\beta_\ell \left[\text{Im}(A_0^L A_\parallel^{L*} - A_0^R A_\parallel^{R*}) + \frac{m_\ell}{\sqrt{q^2}} \text{Im}(A_\perp^L A_S^* - A_\perp^{R*} A_S) \right], \\ J_8 &= \frac{1}{\sqrt{2}}\beta_\ell^2 [\text{Im}(A_0^L A_\perp^{L*} + A_0^R A_\perp^{R*})], \quad J_9 = \beta_\ell^2 [\text{Im}(A_\parallel^{L*} A_\perp^L + A_\parallel^{R*} A_\perp^R)]. \end{aligned} \quad (49)$$

We do not consider here the CP-violating observables and scalar contributions $A_S \equiv 0$. Following Ref. [28] we choose, first, three natural observables: the differential branching

fraction $d\mathcal{B}/dq^2$, the forward-backward asymmetry A_{FB} and the longitudinal polarization

$$\begin{aligned}\frac{d\Gamma}{dq^2} &= \int d\cos\theta d\cos\theta^* d\chi \frac{d^4\Gamma}{dq^2 d\cos\theta^* d\cos\theta d\chi} = \frac{1}{4} (3J_{1c} + 6J_{1s} - J_{2c} - 2J_{2s}) \\ &= \frac{G_F^2}{(2\pi)^3} \left(\frac{\alpha|\lambda_t|}{2\pi} \right)^2 \frac{|\mathbf{p}_2| q^2 \beta_\ell}{12 m_1^2} \mathcal{H}_{\text{tot}}, \quad \frac{d\mathcal{B}}{dq^2} = \frac{1}{\Gamma_B} \frac{d\Gamma}{dq^2},\end{aligned}\tag{50}$$

$$A_{\text{FB}} = \frac{1}{d\Gamma/dq^2} \left[\int_0^1 - \int_{-1}^0 \right] d\cos\theta \frac{d^2\Gamma}{dq^2 d\cos\theta} = -\frac{3}{4} \frac{J_{6s}}{d\Gamma/dq^2} = -\frac{3}{4} \beta_\ell \frac{\mathcal{H}_P^{12}}{\mathcal{H}_{\text{tot}}},\tag{51}$$

$$F_L = -\frac{J_{2c}}{d\Gamma/dq^2} = \frac{1}{2} \beta_\ell^2 \frac{\mathcal{H}_L^{11} + \mathcal{H}_L^{22}}{\mathcal{H}_{\text{tot}}}.\tag{52}$$

Then, inspired by Ref. [10], we introduce the various observables integrated over the relevant kinematic range

$$\begin{aligned}\langle P_1 \rangle_{\text{bin}} &= \frac{1}{2} \frac{\int_{\text{bin}} dq^2 J_3}{\int_{\text{bin}} dq^2 J_{2s}} = -2 \frac{\int_{\text{bin}} dq^2 \beta_\ell^2 f(q^2) [\mathcal{H}_T^{11} + \mathcal{H}_T^{22}]}{\int_{\text{bin}} dq^2 \beta_\ell^2 f(q^2) [\mathcal{H}_U^{11} + \mathcal{H}_U^{22}]}, \\ \langle P_2 \rangle_{\text{bin}} &= \frac{1}{8} \frac{\int_{\text{bin}} dq^2 J_{6s}}{\int_{\text{bin}} dq^2 J_{2s}} = -\frac{\int_{\text{bin}} dq^2 \beta_\ell f(q^2) \mathcal{H}_P^{12}}{\int_{\text{bin}} dq^2 \beta_\ell^2 [\mathcal{H}_U^{11} + \mathcal{H}_U^{22}]}, \\ \langle P_3 \rangle_{\text{bin}} &= -\frac{1}{4} \frac{\int_{\text{bin}} dq^2 J_9}{\int_{\text{bin}} dq^2 J_{2s}} = -\frac{\int_{\text{bin}} dq^2 \beta_\ell^2 f(q^2) [\mathcal{H}_{IT}^{11} + \mathcal{H}_{IT}^{22}]}{\int_{\text{bin}} dq^2 \beta_\ell^2 f(q^2) [\mathcal{H}_U^{11} + \mathcal{H}_U^{22}]}, \\ \langle P'_4 \rangle_{\text{bin}} &= \frac{1}{\mathcal{N}_{\text{bin}}} \int_{\text{bin}} dq^2 J_4 = 2 \frac{\int_{\text{bin}} dq^2 \beta_\ell^2 f(q^2) [\mathcal{H}_I^{11} + \mathcal{H}_I^{22}]}{N_{\text{bin}}}, \\ \langle P'_5 \rangle_{\text{bin}} &= \frac{1}{2\mathcal{N}_{\text{bin}}} \int_{\text{bin}} dq^2 J_5 = -2 \frac{\int_{\text{bin}} dq^2 \beta_\ell f(q^2) [\mathcal{H}_A^{12} + \mathcal{H}_A^{21}]}{N_{\text{bin}}}, \\ \langle P'_6 \rangle_{\text{bin}} &= \frac{-1}{2\mathcal{N}_{\text{bin}}} \int_{\text{bin}} dq^2 J_7 = -2 \frac{\int_{\text{bin}} dq^2 \beta_\ell f(q^2) [\mathcal{H}_{II}^{12} + \mathcal{H}_{II}^{21}]}{N_{\text{bin}}}, \\ \langle P'_8 \rangle_{\text{bin}} &= \frac{-1}{\mathcal{N}_{\text{bin}}} \int_{\text{bin}} dq^2 J_8 = +2 \frac{\int_{\text{bin}} dq^2 \beta_\ell^2 f(q^2) [\mathcal{H}_{IA}^{11} + \mathcal{H}_{IA}^{22}]}{N_{\text{bin}}},\end{aligned}\tag{53}$$

where the normalization \mathcal{N}_{bin} is defined as

$$\begin{aligned}\mathcal{N}_{\text{bin}} &= \sqrt{-\int_{\text{bin}} dq^2 [J_{2s}] \cdot \int_{\text{bin}} dq^2 [J_{2c}]} \\ &= \sqrt{\int_{\text{bin}} dq^2 \beta_\ell^2 f(q^2) [\mathcal{H}_U^{11} + \mathcal{H}_U^{22}] \cdot \int_{\text{bin}} dq^2 \beta_\ell^2 f(q^2) [\mathcal{H}_L^{11} + \mathcal{H}_L^{22}]}. \end{aligned}\tag{54}$$

We also use the phase space factor $f(q^2) = |\mathbf{p}_2| q^2 \beta_\ell$ in the numerator and denominator when calculating the q^2 -averages.

One should notice that the observables P_i are linked to the full four-fold distribution Eq. (46), because the corresponding helicity amplitudes (or equivalent J_i coefficients) do not appear in the single or double differential distributions Eqs. (41) and (40).

VI. NUMERICAL RESULTS

In this section we present the numerical results obtained for various physical observables. The values of the lepton and meson masses and the B-meson lifetime are taken from Ref. [73]. The SM Wilson coefficients are taken from Ref. [10]. They were computed at the matching scale $\mu_0 = 2M_W$ and run down to the hadronic scale $\mu_b = 4.8$ GeV. The evolution of couplings and current quark masses proceeds analogously. The values of the model independent input parameters and the Wilson coefficients are listed in Table IV.

TABLE IV: Values of the input parameters and the corresponding values of the Wilson coefficients used in the numerical calculations.

m_W	$\sin^2 \theta_W$	$\alpha(M_Z)$	\bar{m}_c	\bar{m}_b	\bar{m}_t	$\lambda_t = V_{ts}^\dagger V_{tb} $			
80.41 GeV	0.2313	1/128.94	1.27 GeV	4.68 GeV	173.3 GeV	0.041			
C_1	C_2	C_3	C_4	C_5	C_6	C_7^{eff}	C_9	C_{10}	
-0.2632	1.0111	-0.0055	-0.0806	0.0004	0.0009	-0.2923	4.0749	-4.3085	

In Table V we give the numerical values for the total branching ratios and compare them with available experimental data.

In Figs. 7, 8 and 9 we display our results for the differential decay widths, the forward-backward asymmetry and the longitudinal polarization for the decay $B \rightarrow K^* \ell^+ \ell^-$ in the full kinematical region. We also plot unintegrated clean observables P_i in Figs. 10 and 11. The q^2 -averages of all polarization observables are given in Table VI.

Finally, we present our results for the binned observables in Tables VII and VIII. The binning is chosen to match the current experimental data [81–83] and the results from other

TABLE V: Total branching fractions.

Mode	Our	Others	Expt. [73–75]
$B \rightarrow K^* \mu^+ \mu^-$	12.7×10^{-7}	$(11.9 \pm 3.9) \times 10^{-7}$ [76] 19×10^{-7} [77] 11.5×10^{-7} [78] 14×10^{-7} [79]	$(9.24 \pm 0.93(\text{stat}) \pm 0.67(\text{sys})) \times 10^{-7}$
$B \rightarrow K^* \tau^+ \tau^-$	1.35×10^{-7}	1.9×10^{-7} [77] 1.0×10^{-7} [78] 2.2×10^{-7} [79]	—
$B \rightarrow K^* \gamma$	3.74×10^{-5}	11.4×10^{-5} [80] 4.2×10^{-5} [78]	$(4.21 \pm 0.18) \times 10^{-5}$
$B \rightarrow K^* \nu \bar{\nu}$	1.36×10^{-5}	1.5×10^{-5} [78]	—
$B \rightarrow K \mu^+ \mu^-$	7.18×10^{-7}	5.7×10^{-7} [77] $(3.5 \pm 1.2) \times 10^{-7}$ [76] 4.4×10^{-7} [78] 5×10^{-7} [79]	$(4.29 \pm 0.07(\text{stat}) \pm 0.21(\text{sys})) \times 10^{-7}$
$B \rightarrow K \tau^+ \tau^-$	3.0×10^{-7}	1.3×10^{-7} [77] 1.0×10^{-7} [78] 1.3×10^{-7} [79]	—
$B \rightarrow K \nu \bar{\nu}$	0.60×10^{-5}	0.56×10^{-5} [78]	—

theoretical approaches [10].

The q^2 -integrated predictions and measurements ($1 - 6 \text{ GeV}^2$) for branching fraction and A_{FB} and F_L observables stand

	Belle [81]	LHCb [82]	CDF [83]	CQM
$\mathcal{B} \times 10^7$	$1.49^{+0.45}_{-0.40} \pm 0.12$	$0.42 \pm 0.06 \pm 0.03$	—	2.58
A_{FB}	$0.26^{+0.27}_{-0.30} \pm 0.07$	$-0.06^{+0.13}_{-0.14} \pm 0.04$	$0.29^{+0.20}_{-0.23} \pm 0.07$	−0.02
F_L	$0.67^{+0.23}_{-0.23} \pm 0.05$	$0.55 \pm 0.10 \pm 0.03$	$0.69^{+0.19}_{-0.21} \pm 0.08$	0.75

Considering the outcoming numbers, it is difficult to make a clear statement about the level of agreement. Clearly, the branching fraction prediction is above both measured values.

$B \rightarrow K^* \ell^+ \ell^-$								
	$\langle A_{FB} \rangle$	$\langle F_L \rangle$	$\langle P_1 \rangle$	$\langle P_2 \rangle$	$\langle P_3 \rangle$	$\langle P'_4 \rangle$	$\langle P'_5 \rangle$	$\langle P'_8 \rangle$
μ	-0.23	0.47	-0.48	-0.31	0.0015	1.01	-0.49	-0.010
τ	-0.18	0.092	-0.74	-0.68	0.00076	1.32	-1.07	-0.0018

TABLE VI: q^2 -averages of polarization observables over the whole allowed kinematic region.

On the other hand one has to note the discrepancy which exists between the experimental values themselves and thus a question mark remains on this issue. Concerning the two other observables, A_{FB} and F_L , the model predictions are in agreement with the experiments (slightly overshooting the F_L value for the LHCb experiment), the measurement errors being however quite important. Basically the same commentary can be made about the results in other bins. It is probably necessary to wait until the measurement errors shrink so that the experiments become more constraining.

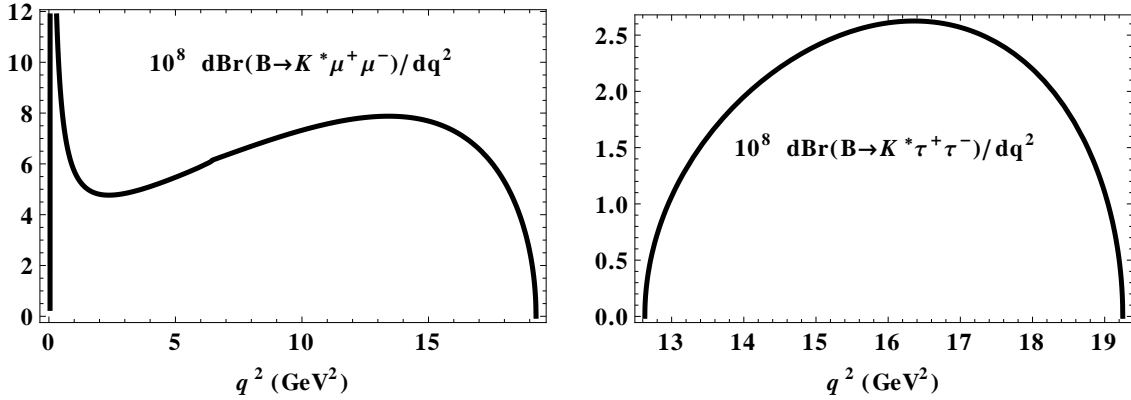


FIG. 7: Differential decay widths of the decays $B \rightarrow K^* \ell^+ \ell^-$.

TABLE VII: Binned observables \mathcal{B} , F_L and A_{FB} for $B \rightarrow K^* \mu^+ \mu^-$ (CQM - covariant quark model).

Bin (GeV^2)	[81]	[82]	[83]	[10]	CQM
	$\mathcal{B}(10^{-7})$				
1.00–2.00	—	—	—	$0.437^{+0.345+0.026}_{-0.148-0.023}$	0.51
0.00–2.00	$1.46^{+0.40}_{-0.35} \pm 0.11$	$0.61 \pm 0.12 \pm 0.06$	-	$1.446^{+1.537+0.057}_{-0.561-0.054}$	1.40
2.00–4.30	$0.86^{+0.31}_{-0.27} \pm 0.07$	$0.34 \pm 0.09 \pm 0.02$	-	$0.904^{+0.664+0.061}_{-0.314-0.055}$	1.13
4.30–8.68	$1.37^{+0.47}_{-0.42} \pm 0.39$	$0.69 \pm 0.08 \pm 0.05$	-	$2.674^{+2.326+0.156}_{-0.973-0.145}$	2.67
10.09–12.89	$2.24^{+0.44}_{-0.40} \pm 0.19$	$0.55 \pm 0.09 \pm 0.07$	-	$2.344^{+2.814+0.069}_{-1.100-0.063}$	2.14
14.18–16.00	$1.05^{+0.29}_{-0.26} \pm 0.08$	$0.63 \pm 0.11 \pm 0.05$	-	$1.290^{+2.122+0.013}_{-0.815-0.013}$	1.39
>16.00	$2.04^{+0.27}_{-0.24} \pm 0.16$	$0.50 \pm 0.08 \pm 0.05$	-	$1.450^{+2.333+0.015}_{-0.922-0.015}$	1.71
1.00–6.00	$1.49^{+0.45}_{-0.40} \pm 0.12$	$0.42 \pm 0.06 \pm 0.03$	-	$2.155^{+1.646+0.138}_{-0.742-0.123}$	2.58
	A_{FB}				
1.00–2.00	—	—	—	$-0.212^{+0.11+0.014}_{-0.144-0.015}$	-0.15
0.00–2.00	$0.47^{+0.26}_{-0.32} \pm 0.03$	$-0.15 \pm 0.20 \pm 0.06$	$-0.35^{+0.26}_{-0.23} \pm 0.10$	$-0.136^{+0.048+0.016}_{-0.045-0.016}$	-0.12
2.00–4.30	$0.37^{+0.25}_{-0.24} \pm 0.10$	$0.05^{+0.16}_{-0.20} \pm 0.04$	$0.29^{+0.32}_{-0.35} \pm 0.15$	$-0.081^{+0.054+0.008}_{-0.068-0.009}$	-0.0059
4.30–8.68	$0.45^{+0.15}_{-0.21} \pm 0.15$	$0.27^{+0.06}_{-0.08} \pm 0.02$	$0.01^{+0.20}_{-0.20} \pm 0.09$	$0.220^{+0.138+0.014}_{-0.112-0.016}$	0.22
10.09–12.89	$0.43^{+0.18}_{-0.20} \pm 0.03$	$0.27^{+0.11}_{-0.13} \pm 0.02$	$0.38^{+0.16}_{-0.19} \pm 0.09$	$0.371^{+0.150+0.010}_{-0.164-0.011}$	0.36
14.18–16.00	$0.70^{+0.16}_{-0.22} \pm 0.10$	$0.47^{+0.06}_{-0.08} \pm 0.03$	$0.44^{+0.18}_{-0.21} \pm 0.10$	$0.404^{+0.199+0.005}_{-0.191-0.005}$	0.36
>16.00	$0.66^{+0.11}_{-0.16} \pm 0.04$	$0.16^{+0.11}_{-0.13} \pm 0.06$	$0.65^{+0.17}_{-0.18} \pm 0.16$	$0.360^{+0.205+0.004}_{-0.172-0.005}$	0.29
1.00–6.00	$0.26^{+0.27}_{-0.30} \pm 0.07$	$-0.06^{+0.13}_{-0.14} \pm 0.04$	$0.29^{+0.20}_{-0.23} \pm 0.07$	$-0.035^{+0.036+0.008}_{-0.033-0.009}$	0.022
	F_L				
1.00–2.00	—	—	—	$0.605^{+0.179+0.021}_{-0.229-0.024}$	0.78
0.00–2.00	$0.29^{+0.21}_{-0.18} \pm 0.02$	$0.00^{+0.13}_{-0.00} \pm 0.02$	$0.30^{+0.16}_{-0.16} \pm 0.02$	$0.323^{+0.198+0.019}_{-0.178-0.020}$	0.54
2.00–4.30	$0.71^{+0.24}_{-0.24} \pm 0.05$	$0.77 \pm 0.15 \pm 0.03$	$0.37^{+0.25}_{-0.24} \pm 0.10$	$0.754^{+0.128+0.015}_{-0.198-0.018}$	0.79
4.30–8.68	$0.64^{+0.23}_{-0.24} \pm 0.07$	$0.60^{+0.06}_{-0.07} \pm 0.01$	$0.68^{+0.15}_{-0.17} \pm 0.09$	$0.634^{+0.175+0.022}_{-0.216-0.022}$	0.60
10.09–12.89	$0.17^{+0.17}_{-0.15} \pm 0.03$	$0.41 \pm 0.11 \pm 0.03$	$0.47^{+0.14}_{-0.14} \pm 0.03$	$0.482^{+0.163+0.014}_{-0.208-0.013}$	0.42
14.18–16.00	$-0.15^{+0.27}_{-0.23} \pm 0.07$	$0.37 \pm 0.09 \pm 0.05$	$0.29^{+0.14}_{-0.13} \pm 0.05$	$0.396^{+0.141+0.004}_{-0.241-0.004}$	0.36
>16.00	$0.12^{+0.15}_{-0.13} \pm 0.02$	$0.26^{+0.10}_{-0.08} \pm 0.03$	$0.20^{+0.19}_{-0.17} \pm 0.05$	$0.357^{+0.074+0.003}_{-0.133-0.003}$	0.34
1.00–6.00	$0.67^{+0.23}_{-0.23} \pm 0.05$	$0.55 \pm 0.10 \pm 0.03$	$0.69^{+0.19}_{-0.21} \pm 0.08$	$0.703^{+0.149+0.017}_{-0.212-0.019}$	0.75

TABLE VIII: Binned clean observables for $B \rightarrow K^* \mu^+ \mu^-$ (our numbers (CQM) vs. reference [10]).

Bin (GeV ²)	[10]	CQM	[10]	CQM
	$\langle P_1 \rangle$		$\langle P_2 \rangle$	
1–2	$0.007^{+0.008+0.054}_{-0.005-0.051}$	−0.0115773	$0.399^{+0.022+0.006}_{-0.023-0.008}$	0.47
0.1–2	$0.007^{+0.007+0.043}_{-0.004-0.044}$	0.0108792	$0.172^{+0.009+0.018}_{-0.009-0.018}$	0.22
2.00–4.30	$-0.051^{+0.010+0.045}_{-0.009-0.045}$	−0.266563	$0.234^{+0.058+0.015}_{-0.085-0.016}$	0.019
4.30–8.68	$-0.117^{+0.002+0.056}_{-0.002-0.052}$	−0.372456	$-0.407^{+0.048+0.008}_{-0.037-0.006}$	−0.37
10.09–12.89	$-0.181^{+0.278+0.032}_{-0.361-0.029}$	−0.470412	$-0.481^{+0.08+0.003}_{-0.005-0.002}$	−0.41
14.18–16.00	$-0.352^{+0.696+0.014}_{-0.467-0.015}$	−0.614669	$-0.449^{+0.136+0.004}_{-0.041-0.004}$	−0.38
16.00–19	$-0.603^{+0.589+0.009}_{-0.315-0.009}$	−0.777736	$-0.374^{+0.151+0.004}_{-0.126-0.004}$	−0.30
1.00–6.00	$-0.055^{+0.009+0.040}_{-0.008-0.042}$	−0.26338	$0.084^{+0.057+0.019}_{-0.076-0.019}$	−0.060
	$\langle P_3 \rangle$		$\langle P'_4 \rangle$	
1–2	$-0.003^{+0.001+0.027}_{-0.002-0.024}$	0.00435836	$-0.160^{+0.040+0.013}_{-0.031-0.013}$	0.14
0.1–2	$-0.002^{+0.001+0.02}_{-0.001-0.023}$	0.00159832	$-0.342^{+0.026+0.018}_{-0.019-0.017}$	−0.15
2.00–4.30	$-0.004^{+0.001+0.022}_{-0.003-0.022}$	0.00454996	$0.569^{+0.070+0.020}_{-0.059-0.021}$	0.89
4.30–8.68	$-0.001^{+0.000+0.027}_{-0.001-0.027}$	0.00224737	$1.003^{+0.014+0.024}_{-0.015-0.029}$	1.13
10.09–12.89	$0.003^{+0.000+0.014}_{-0.001-0.015}$	0.00151139	$1.082^{+0.140+0.014}_{-0.144-0.017}$	1.21
14.18–16.00	$0.004^{+0.000+0.002}_{-0.001-0.002}$	0.00101528	$1.161^{+0.190+0.007}_{-0.332-0.007}$	1.27
16.00–19	$0.003^{+0.001+0.001}_{-0.001-0.001}$	0.00068909	$1.263^{+0.119+0.004}_{-0.248-0.004}$	1.33
1.00–6.00	$-0.003^{+0.001+0.020}_{-0.002-0.022}$	0.00355465	$0.555^{+0.065+0.018}_{-0.055-0.019}$	0.83
	$\langle P'_5 \rangle$		$\langle P'_8 \rangle$	
1–2	$0.387^{+0.047+0.014}_{-0.063-0.015}$	0.258474	—	−0.039
0.1–2	$0.533^{+0.028+0.017}_{-0.036-0.020}$	0.495414	—	−0.033
2.00–4.30	$-0.334^{+0.095+0.02}_{-0.111-0.019}$	−0.423802	—	−0.026
4.30–8.68	$-0.872^{+0.043+0.03}_{-0.029-0.029}$	−0.704599	—	−0.011
10.09–12.89	$-0.893^{+0.223+0.018}_{-0.110-0.017}$	−0.697185	—	−0.0060
14.18–16.00	$-0.779^{+0.328+0.010}_{-0.363-0.009}$	−0.600105	—	−0.0029
16.00–19	$-0.601^{+0.282+0.008}_{-0.367-0.007}$	−0.449369	—	−0.0015
1.00–6.00	$-0.349^{+0.086+0.019}_{-0.098-0.017}$	−0.394563	—	−0.023

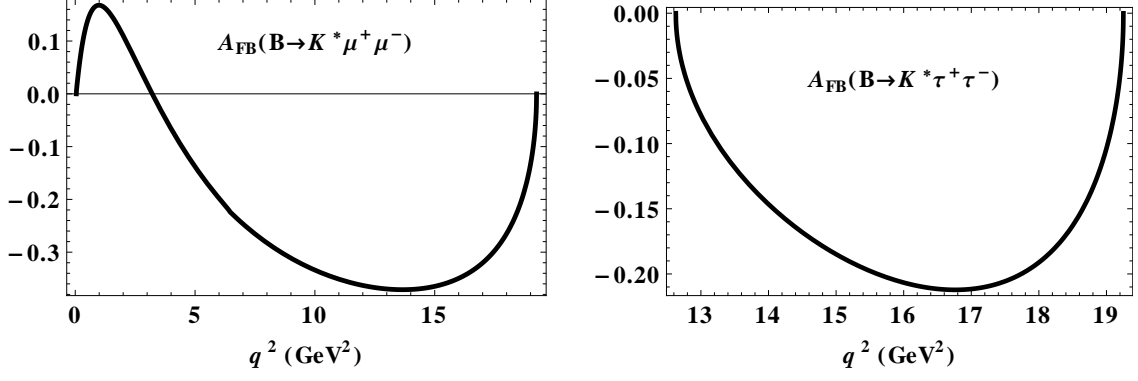


FIG. 8: Forward-backward asymmetry for the decays $B \rightarrow K^* \ell^+ \ell^-$.

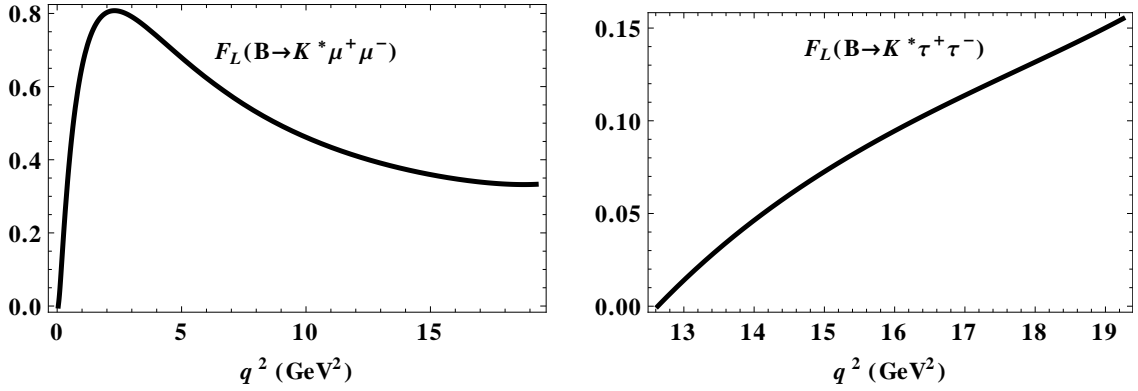


FIG. 9: Longitudinal polarization for the decays $B \rightarrow K^* \ell^+ \ell^-$.

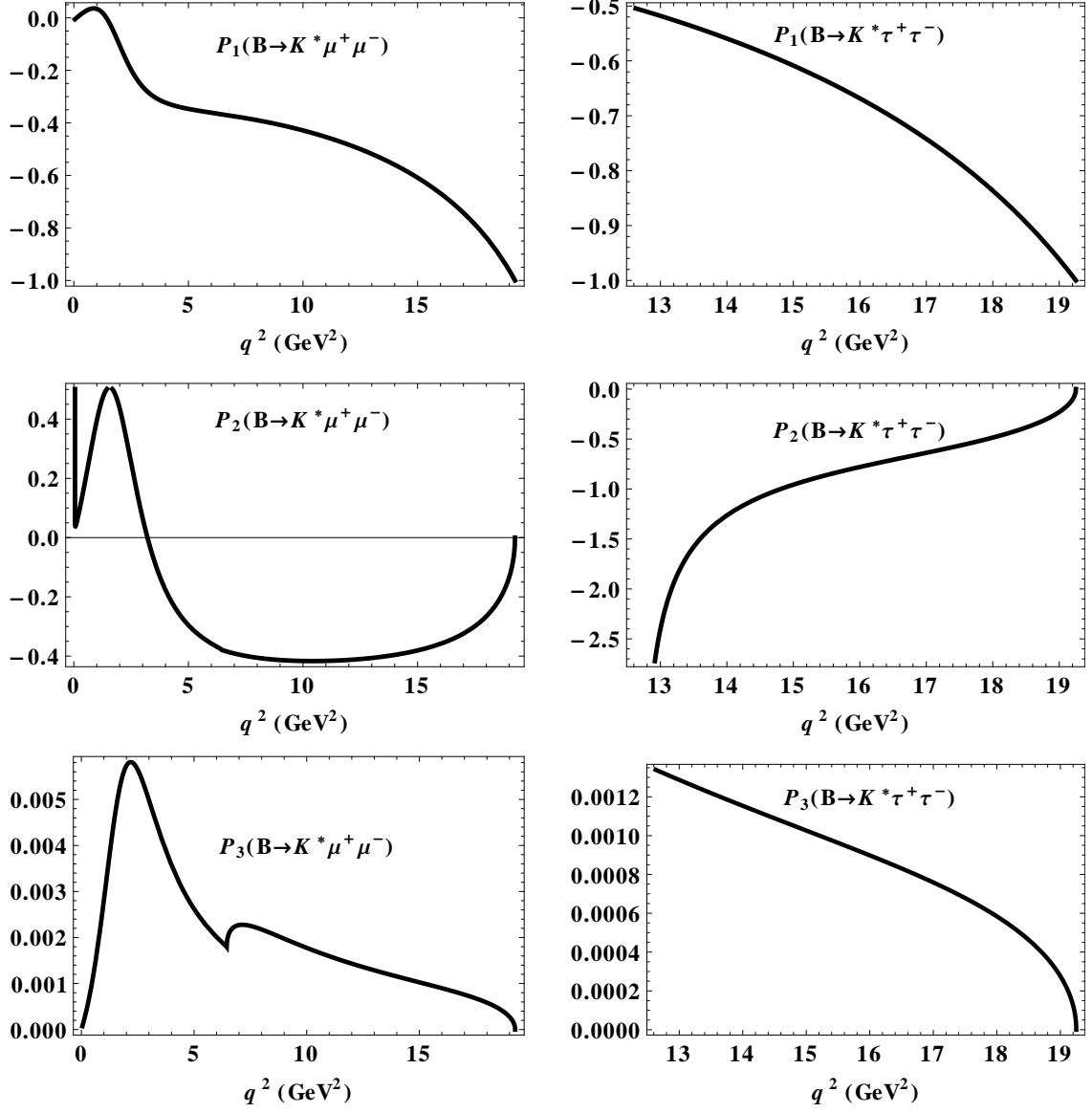


FIG. 10: Clean observables $P_{1,2,3}$ for the decays $B \rightarrow K^* \ell^+ \ell^-$.

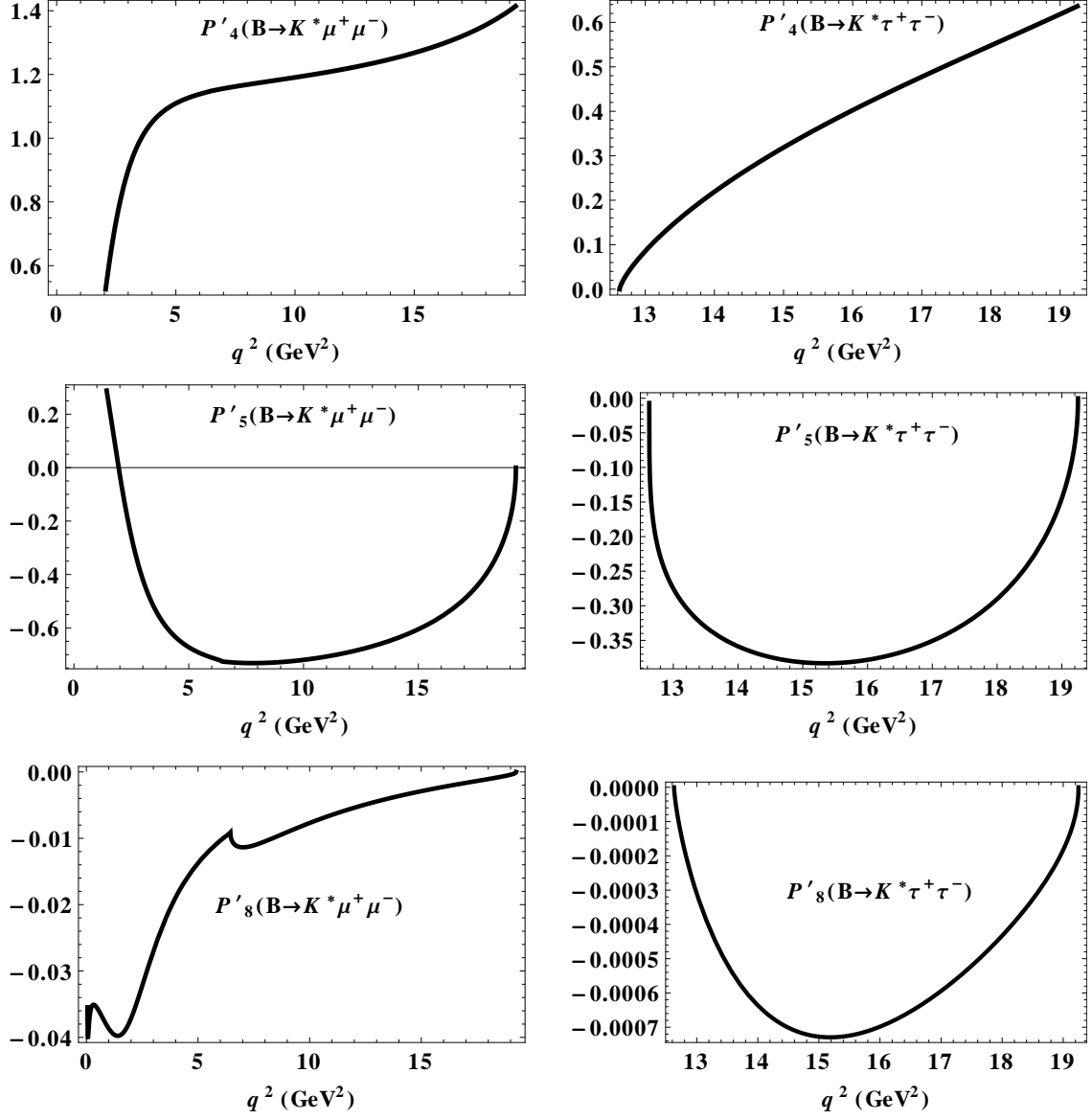


FIG. 11: Clean observables $P'_{4,5,8}$ for the decays $B \rightarrow K^* \ell^+ \ell^-$.

VII. SUMMARY

We have performed a detailed analysis of the decay process $B \rightarrow K^*(\rightarrow K\pi)\bar{\ell}\ell$ in the framework of the covariant quark model by using the helicity formalism to analyze the angular decay distribution. All physical observables have been expressed in terms of the helicity structure functions with taking into account the effects of the finite lepton masses. We have found explicit relations between our helicity formalism and the approach based on the transversality amplitudes which is widely used by both experimentalists and theorists. We have reported our numerical results on the branching fractions, forward-backward asymmetry, longitudinal polarization and a set of the so-called “clean” observables P_i which depend on the hadron uncertainties (form factors) in a minimal way. Finally, we have compared the obtained results with available experimental data and the results from other theoretical approaches.

Acknowledgments

We would like to thank our collaborators Th. Gutsche, J.G. Körner, V.E. Lyubovitskij and P. Santorelli for useful remarks and discussions.

The work was also partly supported by Slovak Grant Agency for Sciences VEGA, grant No. 1/0158/13 (S. Dubnička, A.Z. Dubničková, A. Liptaj), by Slovak Research and Development Agency APVV, grant No. APVV-0463-12 (S. Dubnička, A.Z. Dubničková, A. Liptaj) and by Joint research project of Institute of Physics, SAS and Bogoliubov Laboratory of Theoretical Physics, JINR, No. 01-3-1114 (S. Dubnička, A.Z. Dubničková, M.A. Ivanov and A. Liptaj).

-
- [1] C. Langenbruch [LHCb Collaboration], “Latest results on rare decays from LHCb,” arXiv:1505.04160 [hep-ex].
 - [2] A. Crivellin, J. Heeck and P. Stoffer, arXiv:1507.07567 [hep-ph].
 - [3] J. Lees *et al.* (BABAR Collaboration), Phys. Rev. Lett. **109**, 101802 (2012). arXiv:1205.5442 [hep-ex].
 - [4] M. Tanaka and R. Watanabe, Phys. Rev. D **82**, 034027 (2010) [arXiv:1005.4306 [hep-ph]].

- [5] S. Fajfer, J. F. Kamenik, and I. Nisandzic, Phys. Rev. D **85**, 094025 (2012). arXiv:1203.2654 [hep-ph].
- [6] J. F. Kamenik and F. Mescia, Phys. Rev. D **78**, 014003 (2008). arXiv:0802.3790 [hep-ph].
- [7] R. Aaij *et al.* [LHCb Collaboration], Phys. Rev. Lett. **113**, 151601 (2014) [arXiv:1406.6482 [hep-ex]].
- [8] R. Aaij *et al.* [LHCb Collaboration], Phys. Rev. Lett. **111**, 191801 (2013) [arXiv:1308.1707 [hep-ex]].
- [9] S. Descotes-Genon, J. Matias and J. Virto, Phys. Rev. D **88**, 074002 (2013) [arXiv:1307.5683 [hep-ph]].
- [10] S. Descotes-Genon, T. Hurth, J. Matias and J. Virto, JHEP **1305**, 137 (2013) [arXiv:1303.5794 [hep-ph]].
- [11] T. Hurth and F. Mahmoudi, JHEP **1404**, 097 (2014) [arXiv:1312.5267 [hep-ph]].
- [12] C. Bobeth, G. Hiller and D. van Dyk, JHEP **1007**, 098 (2010) [arXiv:1006.5013 [hep-ph]].
- [13] C. Bobeth, G. Hiller and D. van Dyk, Phys. Rev. D **87**, no. 3, 034016 (2013) [arXiv:1212.2321 [hep-ph]].
- [14] G. Hiller and R. Zwicky, JHEP **1403**, 042 (2014) [arXiv:1312.1923 [hep-ph]].
- [15] J. Gratex, M. Hopfer and R. Zwicky, arXiv:1506.03970 [hep-ph].
- [16] D. Das, G. Hiller, M. Jung and A. Shires, JHEP **1409**, 109 (2014) [arXiv:1406.6681 [hep-ph]].
- [17] L. Hofer and J. Matias, arXiv:1502.00920 [hep-ph].
- [18] S. Descotes-Genon and J. Virto, JHEP **1504**, 045 (2015) [arXiv:1502.05509 [hep-ph]].
- [19] S. Descotes-Genon, J. Matias, M. Ramon and J. Virto, JHEP **1301**, 048 (2013) [arXiv:1207.2753 [hep-ph]].
- [20] W. Altmannshofer and D. M. Straub, Eur. Phys. J. C **73**, 2646 (2013) [arXiv:1308.1501 [hep-ph]].
- [21] R. Mandal, R. Sinha, and D. Das, Phys. Rev. D **90**, 096006 (2014) [arXiv:1409.3088 [hep-ph]].
- [22] J.G. Körner, G.A. Schuler: Z. Phys. C **38** (1988) 511 [Erratum-ibid. C **41** (1989) 690]; Z. Phys. C **46** (1990) 93.
- [23] D. Melikhov, N. Nikitin and S. Simula, Phys. Lett. B **442**, 381 (1998) [hep-ph/9807464].
- [24] F. Kruger, L. M. Sehgal, N. Sinha and R. Sinha, Phys. Rev. D **61**, 114028 (2000) [Erratum-ibid. D **63**, 019901 (2001)] [hep-ph/9907386].
- [25] C. S. Kim, Y. G. Kim, C. D. Lu and T. Morozumi, Phys. Rev. D **62**, 034013 (2000)

- [hep-ph/0001151].
- [26] F. Kruger and J. Matias, Phys. Rev. D **71**, 094009 (2005) [hep-ph/0502060].
 - [27] F. Kruger and L. M. Sehgal, Phys. Lett. B **380**, 199 (1996) [hep-ph/9603237].
 - [28] J. Matias, F. Mescia, M. Ramon and J. Virto, JHEP **1204**, 104 (2012) [arXiv:1202.4266 [hep-ph]].
 - [29] U. Egede, T. Hurth, J. Matias, M. Ramon and W. Reece, JHEP **1010**, 056 (2010) [arXiv:1005.0571 [hep-ph]].
 - [30] M. Beneke, T. Feldmann and D. Seidel, Nucl. Phys. B **612**, 25 (2001) [hep-ph/0106067].
 - [31] H. H. Asatryan, H. M. Asatrian, C. Greub and M. Walker, Phys. Rev. D **65**, 074004 (2002) [hep-ph/0109140].
 - [32] C. H. Chen and C. Q. Geng, Phys. Rev. D **63**, 114025 (2001) [hep-ph/0103133].
 - [33] C. H. Chen and C. Q. Geng, Nucl. Phys. B **636**, 338 (2002) [hep-ph/0203003].
 - [34] A. Ali and A. S. Safir, Eur. Phys. J. C **25**, 583 (2002) [hep-ph/0205254].
 - [35] T. Feldmann and J. Matias, JHEP **0301**, 074 (2003) [hep-ph/0212158].
 - [36] P. Ball and R. Zwicky, Phys. Rev. D **71**, 014029 (2005) [hep-ph/0412079].
 - [37] A. Khodjamirian, T. Mannel and N. Offen, Phys. Rev. D **75**, 054013 (2007) [hep-ph/0611193].
 - [38] M. A. Ivanov, Y. L. Kalinovsky, P. Maris and C. D. Roberts, Phys. Rev. C **57**, 1991 (1998) [nucl-th/9711023].
 - [39] M. A. Ivanov, J. G. Körner, S. G. Kovalenko and C. D. Roberts, Phys. Rev. D **76**, 034018 (2007) [nucl-th/0703094].
 - [40] D. Ebert, R. N. Faustov and V. O. Galkin, Phys. Rev. D **82**, 034032 (2010) [arXiv:1006.4231 [hep-ph]].
 - [41] A. Khodjamirian, T. Mannel, A. A. Pivovarov and Y.-M. Wang, JHEP **1009**, 089 (2010) [arXiv:1006.4945 [hep-ph]].
 - [42] A. K. Alok, A. Dighe, D. Ghosh, D. London, J. Matias, M. Nagashima and A. Szyrkman, JHEP **1002**, 053 (2010) doi:10.1007/JHEP02(2010)053 [arXiv:0912.1382 [hep-ph]].
 - [43] M. Beylich, G. Buchalla and T. Feldmann, Eur. Phys. J. C **71** (2011) 1635 doi:10.1140/epjc/s10052-011-1635-0 [arXiv:1101.5118 [hep-ph]].
 - [44] X. W. Kang, B. Kubis, C. Hanhart and U. G. Meißner, Phys. Rev. D **89**, 053015 (2014) doi:10.1103/PhysRevD.89.053015 [arXiv:1312.1193 [hep-ph]].
 - [45] J. Lyon and R. Zwicky, arXiv:1406.0566 [hep-ph].

- [46] A. Bharucha, D. M. Straub and R. Zwicky, arXiv:1503.05534 [hep-ph].
- [47] C. Greub, V. Pilipp and C. Schubach, JHEP **0812**, 040 (2008) [arXiv:0810.4077 [hep-ph]].
- [48] S. Descotes-Genon, L. Hofer, J. Matias and J. Virto, arXiv:1510.04239 [hep-ph].
- [49] A. Faessler, T. Gutsche, M. A. Ivanov, J. G. Körner and V. E. Lyubovitskij, Eur. Phys. J. direct C **4**, 18 (2002) [hep-ph/0205287].
- [50] T. Branz, A. Faessler, T. Gutsche, M. A. Ivanov, J. G. Körner, V. E. Lyubovitskij, Phys. Rev. D **81**, 034010 (2010). [arXiv:0912.3710 [hep-ph]].
- [51] M. A. Ivanov, J. G. Körner, S. G. Kovalenko, P. Santorelli and G. G. Saidullaeva, Phys. Rev. D **85**, 034004 (2012) [arXiv:1112.3536 [hep-ph]].
- [52] S. Dubnička, A. Z. Dubničková, M. A. Ivanov and A. Liptaj, Phys. Rev. D **87**, 074201 (2013) [arXiv:1301.0738 [hep-ph]].
- [53] A. Issadykov, M. A. Ivanov and S. K. Sakhiyev, Phys. Rev. D **91**, no. 7, 074007 (2015) [arXiv:1502.05280 [hep-ph]].
- [54] T. Gutsche, M. A. Ivanov, J. G. Körner, V. E. Lyubovitskij and P. Santorelli, Phys. Rev. D **86**, 074013 (2012) [arXiv:1207.7052 [hep-ph]].
- [55] T. Gutsche, M. A. Ivanov, J. G. Körner, V. E. Lyubovitskij and P. Santorelli, Phys. Rev. D **87**, 074031 (2013) [arXiv:1301.3737 [hep-ph]].
- [56] T. Gutsche, M. A. Ivanov, J. G. Körner, V. E. Lyubovitskij and P. Santorelli, Phys. Rev. D **88**, no. 11, 114018 (2013) [arXiv:1309.7879 [hep-ph]].
- [57] T. Gutsche, M. A. Ivanov, J. G. Körner, V. E. Lyubovitskij and P. Santorelli, Phys. Rev. D **90**, no. 11, 114033 (2014) [arXiv:1410.6043 [hep-ph]].
- [58] T. Gutsche, M. A. Ivanov, J. G. Körner, V. E. Lyubovitskij, P. Santorelli and N. Haby, Phys. Rev. D **91**, no. 7, 074001 (2015) [arXiv:1502.04864 [hep-ph]].
- [59] S. Dubnička, A. Z. Dubničková, M. A. Ivanov and J. G. Körner, Phys. Rev. D **81**, 114007 (2010) [arXiv:1004.1291 [hep-ph]].
- [60] S. Dubnička, A. Z. Dubničková, M. A. Ivanov, J. G. Koerner, P. Santorelli, G. G. Saidullaeva, Phys. Rev. **D84**, 014006 (2011). [arXiv:1104.3974 [hep-ph]].
- [61] M. Dineykhani, M. A. Ivanov and G. G. Saidullaeva, Phys. Part. Nucl. **43**, 749 (2012).
- [62] G. V. Efimov and M. A. Ivanov, Int. J. Mod. Phys. A **4**, 2031 (1989).
- [63] G. V. Efimov and M. A. Ivanov, *The Quark Confinement Model of Hadrons*, (CRC Press, Boca Raton, 1993).

- [64] S. Weinberg, Phys. Rev. **130**, 776 (1963).
- [65] A. Salam, Nuovo Cimento **25**, 224 (1962).
- [66] K. Hayashi, M. Hirayama, T. Muta, N. Seto, and T. Shirafuji, Fortsch. Phys. **15**, 625 (1967).
- [67] J. A. M. Vermaseren, Nucl. Phys. Proc. Suppl. **183**, 19 (2008) [arXiv:0806.4080 [hep-ph]]; arXiv:math-ph/0010025.
- [68] D. Ebert, T. Feldmann and H. Reinhardt, Phys. Lett. B **388**, 154 (1996) [arXiv:hep-ph/9608223].
- [69] M. A. Bedolla, J. J. Cobos-Martinez and A. Bashir, Phys. Rev. D **92**, no. 5, 054031 (2015).
- [70] G. Ganbold, T. Gutsche, M. A. Ivanov and V. E. Lyubovitskij, J. Phys. G **42**, no. 7, 075002 (2015) [arXiv:1410.3741 [hep-ph]].
- [71] G. Buchalla, A. J. Buras and M. E. Lautenbacher, Rev. Mod. Phys. **68**, 1125 (1996) [hep-ph/9512380].
- [72] A. Ali, T. Mannel, T. Morozumi: Phys. Lett. B **273** 505 (1991).
- [73] K. A. Olive *et al.* [Particle Data Group Collaboration], Chin. Phys. C **38**, 090001 (2014).
- [74] R. Aaij *et al.* [LHCb Collaboration], JHEP **1406**, 133 (2014) [arXiv:1403.8044 [hep-ex]].
- [75] L. Pescatore [LHCb Collaboration], “Rare decays at the LHCb experiment,” arXiv:1410.2411 [hep-ex].
- [76] A. Ali, E. Lunghi, C. Greub and G. Hiller, Phys. Rev. D **66** (2002) 034002 [hep-ph/0112300].
- [77] A. Ali, P. Ball, L. T. Handoko and G. Hiller, Phys. Rev. D **61** (2000) 074024 [hep-ph/9910221].
- [78] D. Melikhov, N. Nikitin and S. Simula, Phys. Rev. D **57** (1998) 6814 [hep-ph/9711362].
- [79] C. Q. Geng and C. P. Kao, Phys. Rev. D **54** (1996) 5636 [hep-ph/9608466].
- [80] M. A. Ivanov, Y. L. Kalinovsky and C. D. Roberts, Phys. Rev. D **60** (1999) 034018 [nucl-th/9812063].
- [81] **Belle** Collaboration, Phys. Rev. Lett. **103**, 171801 (2009) [arXiv:0904.0770 [hep-ex]].
- [82] **LHCb** Collaboration, Phys. Rev. Lett. **108**, 181806 (2012), [LHCb-CONF-2012-008 and arXiv:1112.3515 [hep-ex]].
- [83] **CDF** Collaboration, Phys. Rev. Lett. **108**, 081807 (2012) [arXiv:1108.0695 [hep-ex]].